NTNU – Trondheim
Norwegian University of
Science and Technology

Space Charge Distribution in Layered XLPE Cable Insulation under HVDC Stress Conditions

Jørn Frøysa Hole

Master of Energy and Environmental Engineering
Submission date: Januar 2015
Supervisor: Frank Mauseth, ELKRAFT
Co-supervisor: Øystein Hestad, SINTEF Energy Research

Norwegian University of Science and Technology
Department of Electric Power Engineering

NTNU
Det skapende universitet

Space Charge Distribution in Layered XLPE Cable Insulation under HVDC Stress Conditions

Jørn Frøysa Hole

Masteroppgave i energi og miljø

Date of Submission: January 18th, 2015

Supervisor: Frank Mauseth, ELKRAFT

Co-Supervisor: Øystein Hestad, SINTEF

Norges Teknisk- Naturvitenskapelige Universitet

Institutt for Elkraftteknikk

Problem Description

Due to the increasing demand for supply of reliable electric power, installations of more high capacity and long distance high voltage DC cable transmissions are required. During the latest decades extruded polymeric insulation has been the dominant choice of insulation for HVAC cable technology and there is a strong incentive to develop and produce HVDC cables with extruded polymeric insulation; cables that offer the same benefits – flexibility, lower weight and cost-effectiveness – as the AC transmission cables.

Cable joints and terminations in a polymeric HVDC insulation system is regarded as the most critical parts of the cable systems. It is desirable to study the space charge distribution within the polymeric HVDC insulation with interfaces, e.g. an insulation system with different polymers, and accordingly the electric field distribution within the entire polymeric insulation system. Knowledge on the role of space charges in insulation systems with interfaces under DC stress is essential when designing HVDC accessories and the Master's thesis will be an important contribution to research and development of cable accessories.

This Master's thesis is mainly experimental, and will consist of measurements on flat samples.

Supervisor: Frank Mauseth, NTNU
Co-supervisor: Øystein L. G. Hestad, SINTEF Energy Research AS

Preface

This thesis is the final work of the Master programme in Electrical Power Engineering at the Norwegian University of Science and Technology.

I would like to thank my supervisor, Professor Frank Mauseth, for guidance and support throughout the work on this thesis, and all the extra hours spent on my behalf. I would also like to thank SINTEF for kindly letting me use their laboratories.

Lastly, I would like to thank all my friends and colleagues here at NTNU, especially my mates at the office, for being supportive, offering help, and lightening the mood.

Abstract

In order to connect offshore installations with maximum effectiveness, high voltage direct current cables are essential. Because of the many benefits of extruded polymer insulation, such as low price and ease of manufacture, improved solutions suitable for higher voltages are ever in demand.

One of the challenges related to HVDC cable installations is high power electrical connectors. Cable joints and terminations are considered critical components in a cable system, and thus demand extensive research and improved knowledge in order to enable the next generation of installations.

Material interfaces are inevitable in connectors, and the aim of this Master's Thesis is to examine the space charge accumulation and field development in insulation containing a material interface under DC stress. This has been done through experimental work, applying voltage to layered samples consisting of a polymeric insulation material developed in particular for use in HVDC installations, and measuring the resulting development of space charge and field distribution. The samples consisted of one cross-linked layer cross-linked once again with another layer of the same material, mimicking the interface created in connections.

The space charge distribution has been measured using the *Pulsed Electroacoustic Method* for flat specimens. Measurements have been performed with an average field stress of 20, 30 and 40kV/mm, and a duration of 8 to 19 days. Two series of measurements have been conducted on layered samples with a field of 30kV/mm, in order to examine reproducibility, and one series of measurements has been performed on a single-layer sample with a field of 30kV/mm as a reference. In order to examine a possible difference in the conductivity of the layers, the degree of crystallinity of layered and unlayered samples has been measured. Since there is a strong correlation between the degree of crystallinity and conductivity, this could give a good indication of possible differences.

No particular accumulation of charge was observed in the interface of the samples, indicating no increased risk in interfaces between double cross-linked and cross-linked polymer of the material examined. The degree of crystallinity of the layered and unlayered samples was similar, indicating that no charge would build due to a difference in conductivity, and supporting the PEA measurements.

Accumulated hetero charge in the polymer close to the anode, unrelated to the material interface, caused a significant increase in field strength on the anode side of the samples. The accumulations of hetero charge in the samples stabilised in all of the samples, reaching stability faster with a stronger applied field. The amount of charge also showed a positive correlation with the applied field. This development can in all likelihood be ascribed to the hetero charges' positive influence on the field strength, combined with the field's lowering of the potential barrier for electron extraction at

the anode. As these mechanisms reach equilibrium, stability is attained. The reason for the hetero charge accumulation in the first place can probably be attributed to *Schottky injection* of electrons at the cathode, in combination with a faster rate of electron transport in the polymer. In accordance with the hetero charge in the polymer by the anode, positive charge accumulated at both electrode-polymer interfaces.

The distribution of charge accumulation in the rest of the bulk of the material showed no reliable trends throughout the measurements, except for a tendency towards negative net charge, indicating trapping of electrons in the polymer bulk.

In addition to the mechanisms mentioned, ions may have contributed to charge accumulation, but given the results obtained, no definitive conclusion can be made with regards to this possibility.

Earlier examinations of samples without interfaces have obtained similar results, supporting the conclusion that an interface of the kind examined has little to no effect on the accumulation of charge.

Sammendrag

For å koble offshoreinstallasjoner med maksimal effektivitet er høyspente likestrømskabler essensielle, og på grunn av de mange fordelene med ekstrudert polymer-isolasjon, så er det en konstant etterspørsel av forbedrede løsninger for denne isolasjonsløsningen.

En av utfordringene i forbindelse med HVDC kabelinstallasjoner er elektriske koblinger for høy effekt. Kabelskjøter og termineringer er ansett som kritiske punkter i et kabelsystem, og krever derfor omfattende forskning og økt kunnskap for å kunne utvikle neste generasjon av installasjoner.

Grenseflater mellom materialer er uunngåelige i elektriske koblinger, og målet med dette masterarbeidet er å undersøke romladningsakkumulering og feltutvikling i isolasjon med grenseflater som er satt under likespenning. Dette har blitt gjort gjennom eksperimentelt arbeid, der spenning ble påtrykt lagdelte tesobjekter bestående av et polymerisk isolasjonsmateriale utviklet spesielt for bruk i HVDC-installasjoner, og resulterende romladningsfordeling og feltutvikling målt. Testobjektene bestod av et kryssbundet lag kryssbundet på nytt med ett nytt lag av det samme materialet, i etterligning av de grenseflatene en finner i koblinger.

Romladningsdistribusjonen har blitt målt ved *Pulsed Electroacoustic Method* for flate testobjekter. Målinger har blitt utført med påtrykte gjennomsnittsfelt på 20, 30 og 40kV/mm, og en varighet fra 8 til 19 døgn. To serier med målinger ble gjort på lagdelte testobjekter med et påtrykt felt på 30kV/mm, for å undersøke reproduserbarhet, og en måleserie ble utført på et ikke-lagdelt testobjekt ved 30kV/mm som en referanse. For å undersøke mulig forskjell i konduktivitet mellom lagene, har krystallinitetsgraden til lagdelte og ikke-lagdelte tastobjekter blitt målt. Siden det er en sterk korrelasjon mellom krystallinitetsgrad og konduktivitet, kunne dette gi en god indikasjon på eventuelle forskjeller.

Ingen særlig akkumulering av ladninger ble observert i testobjektenes grenseflate, noe som indikerer at det ikke er noen økt risiko i grenseflater mellom dobbelt og enkelt kryssbundet polymer av det undersøkte materialet. Krystallinitetsgraden til objektene var relativt lik, og indikerte dermed at ladning ikke ville akkumuleres på grunn av forskjell i ledeevne, noe som samstemte med PEA målingene.

Akkumulert heteroladning i polymeret nære anoden, urelatert til grenseflaten, forårsaket en betydelig økning i feltstyrke på anodesiden av testobjektene. Akkumuleringen av heteroladninger stabilisertes i alle testobjektene, fortere jo sterkere felt som var påtrykt. Mengden ladning viste også en positiv korrelasjon med påtrykt felt. Denne utviklingen kan sansynnligvis tilskrives heteroladningenes positive innflytelse på feltstyrken, kombinert med at feltet gjør potensialbarrieren for ekstraksjon av electroner ved anoden lavere. Når disse mekanismene når likevekt oppnås stabilitet. Grunnen til at heteroladninger akkumulerte er sannsynligvis på

grunn av *Schottky injeksjon* av elektroner fra katoden, kombinert med en raskere transport av elektroner i polymeren. I henhold til heteroladningen i polymeren ved anoden, ble positiv ladning akkumulert ved begge elektrode-polymer-grenseflatene.

Ladningsdistribusjonen i resten av materialbulken viste ingen tydelige trender på tvers av målingene, med unntak av en tendens mot negativ netto ladning, noe som tyder på elektronfangst i polymerbulken.

I tilleg til de mekanismene som er nevn så kan ioner ha bidratt med ladningsakkumulering, men gitt de oppnådde resultatene kan ingen definitiv konklusjon bli gjort i forbindelse med denne muligheten.

Tidligere undersøkelser av testobjekter uten grenseflater har oppnådd lignende resultater, noe som støtter opp under konklusjonen om at grenseflater av typen som er undersøkt ikke har stor innvirkning på ladningsakkumulering.

Table of Contents

List of Figures

Chapter 1

Introduction

Long distance connections are becoming ever more in demand as the need for a more efficient power system pushes the development of our energy infrastructure. This transition into a more efficient power system is driven by ever stricter regulations and demands for a more sustainable and environmentally friendly development in the means of production, distribution and consummation of energy.

Increasing the share of renewable energy in the power grid is leading to challenges when it comes to the connection of remotely located installations such as offshore wind farms, and less controllable sources of energy calls for a greater integration between power markets in different regions and countries.

The most efficient technology in use today for the transmission of large amounts of power over long distances is high voltage direct current connections. When lines are impractical, HVDC connections through cables are necessary. This technology has been in use since the 1950s, and the most common cable insulation material today is, as it was then, mass impregnated paper [1]. The reason mass impregnated paper has remained so popular is its familiarity and known reliability as an insulating material for high voltages. In the later years, however, cross linked polyethylene (XLPE) has shown ever more promise as a replacement in newer installations. XLPE has a lower weight, is easy to manufacture and splice, and can withstand higher temperatures.

Since the first HVDC project utilising XLPE insulated cables in 1997 in Gotland at 80kV, the voltage level at which XLPE has been used has increased gradually, surpassing 300kV. Even so, there is much room for improvement, and one of the biggest challenges facing developers of new XLPE HVDC connections today is the accumulation of space charges in the insulation. Space charge can lead to field distortion and accelerated ageing of the material, making it a priority to avoid accumulation in the insulation.

In HVAC transmission lines, the polarity of the voltage is changed continuously, so there is no time for space charges to accumulate. In HVDC transmission, however, the polarity is only changed if the direction of the power flow is changed (In some newer installations, use of power electronics eliminate the need to change polarity in order to change the direction of the power flow), which is far from often enough to prevent space charge accumulation. This creates a constant need to improve the characteristics of the insulation material as higher transmission voltages are opted for.

One potential pitfall when it comes to space charges is related to cable terminations and connections. Since installing long distance cables in one continuous piece is highly

impractical, cable connections are inevitable. At these points, the insulation material of the two cable lengths must be joined, creating an interface in the material. The accumulation of space charges could potentially be much larger at these interfaces than in the general parts of the cable insulation. Common procedure for connecting two parts of insulation is through cross-linking (see section 2.1.2) the parts together. When this is done, one side of the connection will be already cross-linked, while the other is not. Therefore, cross-linking the parts together results in one side being cross-linked while the other is double cross-linked. With this in mind, the accumulation of space charges in such interfaces between two pieces of XLPE insulation has been investigated in this thesis.

Work Previously Done on the Topic

This work is the continuation of the Master's Thesis work done by Jens-Eirik Hagen in 2014 [2], where the accumulation of space charges in high voltage DC insulation was also examined. The emphasis in the thesis was on the accumulation of space charges in the interface between layers of material in the isolation, and their effect on the electric field.

The main experiments on layered insulation done in Hagen's thesis were performed on two types of layered samples. The first type consisted of one layer of AC insulation and one layer of DC insulation, where the AC material was crosslinked twice, and the DC material once. The second type was similar, except that both materials were cross-linked only once. The production of these samples, and measurements performed were done in the same manner as will be described in this thesis.

Chapter 2

Theoretical Background

In order to examine the effect of interfaces between sections of insulation on the accumulation of space charges in cross-linked polyethylene under DC stress, and how these space charges influence the electrical field distribution and the material, it is necessary to have a thorough theoretical understanding of the physical mechanisms at work. First, a consideration of material properties will be presented, followed by a review of the theoretical foundation for field distribution, the injection and transport of space charges, and their influence on each other. Finally, the theory behind the method used for the detection of space charges will be explained.

2.1. Material Properties

A perfect dielectric is an insulating material without any transport of electrons, electron holes (the conceptual and mathematical opposite of an electron) or ions. Although no perfect dielectric exists in reality, there are materials with good dielectric properties which are widely used today. Polymer based dielectrics have a high breakdown voltage ($\sim 10^9 \Omega m^{-1}$), low dielectric losses ($\tan\delta < 10^{-3}$) and a high DC resistance ($\sim 10^{16} \Omega m$), as well as high durability, ease of manufacture and low costs, making them a prime candidate for future installations [3].

The extruded materials used for the insulation of HVDC cables can be divided into two categories: Pure materials and materials with proper additives [1]. Adding other materials to the mix under production can have several beneficial effects on the properties of the insulation. Because of the problems related to space charge accumulation, insulation consisting of pure material has been mostly abandoned in favour of materials with additives.

These additives can be divided into three main categories [3]:

1. Additives used under production and catalysts used under cross-linking. After the production process, remnants of these materials may still be present in the material.
2. Additives used in order to enhance certain traits of the material, such as protection against heating, ultra violet radiation and oxidation.
3. Compounding ingredients, which are added in order to change the behaviour of the material under production and during operation of the cable. Fillers are added in order to reduce costs and improve the mechanical properties and the heat resistance of the material. Softeners are used to reduce the frailty of the dielectric material, and to improve the flow of the material during production.

2.2.1. Polyethylene

Semi-crystalline polyethylene is thermoplastic artificial material produced using gaseous ethen, C_2H_2. In its finished form, polyethylene consists of multiple strains of repeating CH_2-units, with intermittent branches every 30th – 100th repetition. These side chains can cause areas in the material where strains are arranged more haphazardly, so-called amorphous regions. Conversely, the areas where strains are arranged parallel to each other are called crystalline regions. In the amorphous regions, the density of the material is lower, and there is a greater chance of chemical impurities accumulating, causing these regions to have a great influence on the accumulation of space charges and the transport of charges in the material. As mentioned, the arrangement of the polymers influences the density of the material, a higher degree of crystallinity leading to higher density. Polyethylene is therefore often classified as either high density polyethylene (HDPE) or low density polyethylene (LDPE) according to the materials degree of crystallinity. In terms of material characteristics, HDPE is less flexible than LDPE, making LDPE more suitable for cable insulation, but a lower degree of crystallinity also leads to lower resistivity, affecting the accumulation of space charges. An illustration portraying semi-crystalline polyethylene, with crystalline and amorphous regions, is shown below:

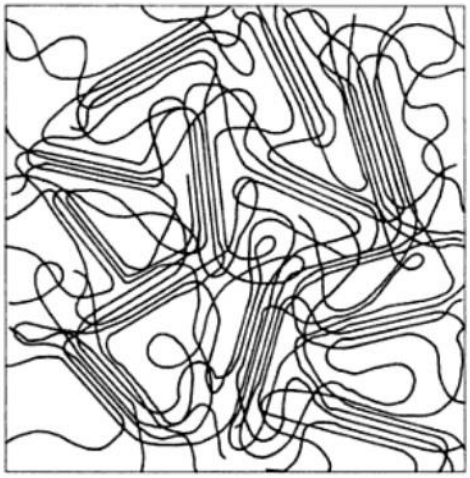

Figure 1: Semi-crystalline polyethylene with crystalline and amorphous regions [3]

2.2.2. Crosslinking

In order to raise the melting point of the insulation material, polyethylene is often cross-linked. This is done through a vulcanisation process where the material is heated under high pressure, causing the strains of polyethylene to form lateral connections, as illustrated below:

Figure 2: Cross-linking of polymers

Crosslinking is also often achieved chemically through the use of peroxides, typically dicumyl peroxide. Residuals from the crosslinking process can influence the material properties and the accumulation of space charges in the material. These are mostly removed by thermal pre-treatment, but depending on the thickness of the sample and the duration of the conditioning, various amounts will remain. Common residuals from crosslinking are methane, acetophenone, and cumyl alcohol.

2.2.3. Material Used In This Work

In the experiments performed during the work on this Master's Thesis, the material used has been a cross-linked polyethylene specifically developed for use in high voltage DC installations.

The name of the insulation material is Borlink LE4253DC. In 2011, the manufacturer Borealis received the Europe Product Leadership Award in HVDC Cable Insulation Market for their work on this material. It was designed with the intent of minimising space charge accumulation, as well as being easy to extrude.

2.2. Conduction

When voltage is applied between two parallel surfaces, the field between the surfaces will in an ideal case be given by the equation

$$E_0 = \frac{U_0}{d} \tag{1}$$

Here, U_0 is the applied voltage, and d is the distance between the surfaces. In a sylindrical configuration, the field is given as a function of the radius (see Section

2.3). Charged particles in a field will experience a force in the field direction equal to the product of the field strength and its charge. A material's ability to not resist this force is the conductivity.

The conductivity of a material given i different charge carriers can be given by:

$$\sigma_i = n_i e_i \mu_i \tag{2}$$

Where n is the concentration, e is the electrical charge [C], and μ is the mobility $[m^2V^{-1}s^{-1}]$ of charge carrier i. As there are several different kinds of charge carriers (electrons, holes, protons, and positive and negative ions), it is more practical to express the conductivity as a sum of multiple mechanisms:

$$\sigma = \sum_{i}^{N} |n_i e_i \mu_i| \tag{3}$$

In most cases, one type of charge carrier will be dominant, and the conductivity can largely be explained by variations in n, e and μ. The variation of e in most solid insulation materials is normally small enough to be of little significance compared to the product of the mobility and the concentration.

2.3. Field Distribution in HVDC Cables

If it were assumed that the conductivity of the insulation in the HVAC cable was independent of temperature and constant throughout the insulation, the resulting calculation would be the same as that for a HVAC cable [1]:

$$E_{AC}(r) = \frac{U_0}{r ln(\frac{r_o}{r_i})} \tag{4}$$

Her, E [V/m] is the electrical field, U [V] is the voltage across the dielectric, r [m] is the radius at the examined position, and r_o and r_i [m] is the outer and inner radius of the dielectric, respectively. This approach is widely used for HVAC considerations since the permittivity is close to unaffected by differing temperatures. This calculation would also be valid for HVDC cables, were the conductivity of the insulation independent of the temperature and field. It is still a quite good approximation for the conditions when the cable is first energised at zero load. As the cable is loaded, and heating of the conductor starts, the DC field develops into a purely resistive distribution which in mathematical terms stabilises as time approaches infinity. In practice, the current density in the insulation will reach its steady state value when a DC voltage has been applied for a long time, and there will be an accumulated space charge present. As shown in page 50 and 51 of [1] this can be proven by considering the relation between the electrical field, current density,

Gauss law for space charge and current continuity. The resulting space charge can be described by the following equation:

$$\boldsymbol{J} \cdot \nabla\left(\frac{\varepsilon_0 \varepsilon_r}{\sigma}\right) = \sigma \boldsymbol{E} \cdot \nabla\left(\frac{\varepsilon}{\sigma}\right) = \rho \tag{5}$$

Where $\boldsymbol{J}$ is the current density, ε_0 and ε_r are the permittivity of free space and the relative permittivity, σ is the conductivity of the dielectric, $\boldsymbol{E}$ is the electric field, and ρ is the space charge density.

The dependence of the conductivity on the field distribution and temperature of the material suggests that the distribution of charge in the insulation will tend to not be uniform. Since the current density is positively correlated to the field strength, the amount of charge in a high-field area will be higher than in low-field areas. The charge accumulation will, as mentioned, reach a point of equilibrium given constant voltage and temperature conditions. For lower temperature drops, the highest charge density will appear close to the conductor [1].

Since the conductivity decreases with r, the resulting charge will have the same sign as the inner electrode, resulting in homo charge in the inner part of the insulation, and hetero charge in the outer part.

The work done in this thesis deals with flat samples of insulation, and so a constant temperature and initial field is assumed, making these considerations not directly relevant. They are, however, something to consider when observations are to be projected onto situations in real cable installations.

2.4. Space Charge Accumulation and Field Distortion

Space charges accumulate when there is an imbalance in the amount of charge carriers transported in and out of an area. This can be expressed through the current continuity equation:

$$\nabla \cdot \vec{j} + \frac{\delta \rho}{\delta t} = 0 \tag{6}$$

Here, j is the current density, ρ is the space charge density, and t is the time. The accumulated charge will introduce a new contribution to the electric field according to Gauss' law:

$$\rho = \nabla \cdot \varepsilon_0 \varepsilon_r \vec{E}_\rho \tag{7}$$

Where ε_0 is the permittivity of free space and ε_r is the relative permittivity of the material. In this case, the total electric field will be the sum of the laplacian field, E_0 and the contribution from the space charges, E_ρ [5]:

$$E = E_0 + E_\rho \tag{8}$$

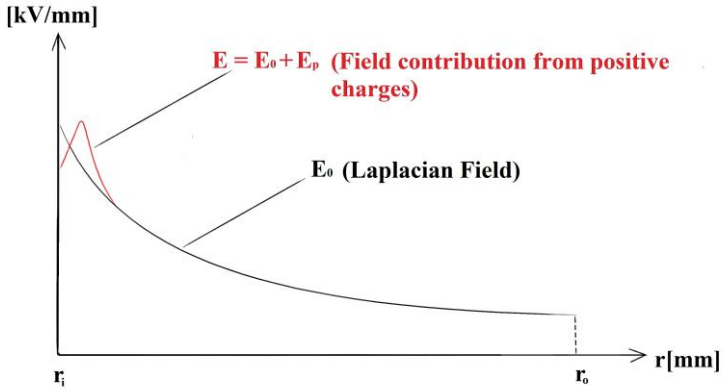

Figure 3: Field influenced by positive charge in a cylindrical configuration

The maximum percentage increase in field strength due to space charges in a flat sample with parallel electrodes can be calculated as

$$F_{E\%} = \frac{E_{max} - \frac{U_0}{d}}{\frac{U_0}{d}} \tag{8}$$

Here, E_{max} is the maximum observed increase in field strength, U_0 is the applied voltage, and d is the thickness of the test object.

2.5. Charge Injection and Transport

Different charge carriers will be active in the transport of charges, depending on the chemical and physical properties of the material, as well as the applied field, temperature and frequency, electrode configuration and moisture. Depending on which carriers are active, the transport can be classified. Typically, a distinction is made between ionic transport and electronic transport.

2.5.1. Energy Bands

In order to understand what is physically happening inside the material as charge is transported, the Niels Bohr model of the atom is a sensible starting point. In an atom, electrons can occupy a limited amount of energy states, and in Niels Bohr's model, this is represented by layered orbits around the atomic nucleus. Given the right addition or subtraction of energy from the electron through electromagnetic radiation, it can jump from one orbit to another. If an outer electron is bound to one

particular nucleus, it is in the so-called valence band, and if it is not, it is in the conductive band. Between these states, there is an energy gap where it is impossible for an electron to be situated, and so the electron or electron hole can only move across this gap if it gains enough energy to completely cross it. The width of this gap band determines the conductivity of a material, seeing as a larger gap makes it harder for an electron to cross into the conductive state. The width of the band gap can be expressed in electron volts [eV]. For insulators, the band gap is larger than 2 eV, for a semi-conductor it is between 0,2 and 1 eV, and for a conductor it is smaller than 0,2 eV [3, 6].

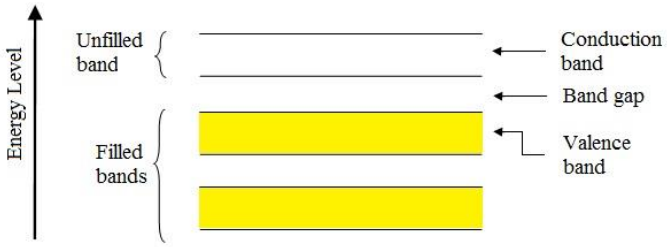

Figure 4: Semiconductor Band Structure

Incompletely bound atoms in crystal defects create free connections which can be satisfied either by the removal or donation of an electron (or both), and therefore work as states in the band gap. States of this kind are found in the vicinity of chemical or structural defects in the material, often in amorphous regions. Electrons and holes in these localised states are not available for conduction, and require significant amounts of energy in order to exit their current state. For this reason, these incompletely bound atoms are known as traps. Where an electron is trapped, the term acceptor is often used, while traps for holes are called donors. Donors have energy levels just above the top of the valence band, while acceptors have energy levels just below the bottom of the conductive band [3].

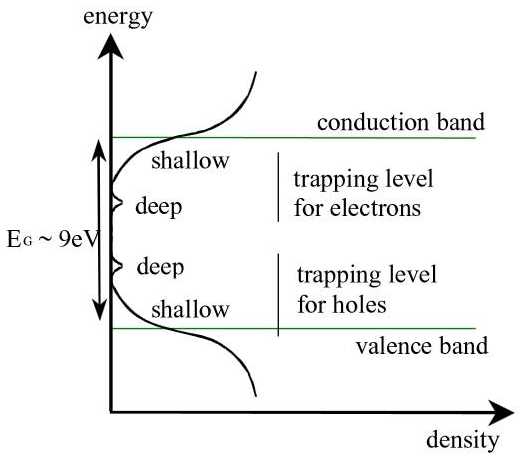

Figure 5: Schematic representation of state density in a disordered dielectric material [1]

A trapped electron or hole can reorient the local structure and thus create a potential well making escape difficult. These potential wells are called self-traps, and are traps where a space charge of one polarity in a region is not compensated by space charge of the opposite polarity. This leads to a localised field increase which can be calculated by Poisson's equation [3]:

$$\nabla E = \frac{\rho_c}{\epsilon} \tag{9}$$

Here, ρ_c is the space charge density (Cm^{-3}), and ϵ is the permittivity. Self-traps can be deep, and are able to keep charge for periods from a few hours up to days.

The occurrence of traps is strongly related to the additives in the polymer, and small variations can have a large impact on the amount of traps present.

2.5.2. Ionic Transport

Electrically charged atoms are known as ions, and in polymer insulation, they are inclined to be created in the interface between the insulation and electrodes, as well as in the bulk of the material due to disassociation of impurities and chemical additives. When charge is transported in the form of ions, it is also simultaneously a transport of mass, and since the electrodes are only able to inject and extract electrons, ionic transport cannot continue perpetually without the formation of new ions [3]. Ionic transport can be divided into two categories:

1. Inner ionic conduction caused by the dissociation of the main molecule or side groups followed by the transfer of protons and/or electrons through hydrogen bound networks.
2. Outer ionic conduction caused by impurities or chemical additives which are not a part of the chemical structure of polymer.

2.5.3. Electronic Transport

Electrons can be trapped by acceptors or ionised donors, while holes can be trapped by donors or ionised acceptors. In order to leave traps, the charges have to surmount large potential barriers through thermal excitation. According to the *Poole-Frenkel mechanism,* higher fields reduce the barriers that lock charge carriers within the dielectric [1], thus assisting thermally activated hopping. In thermally activated hopping, charge carriers gain enough energy to pass the potential barrier through thermal kinetic energy.

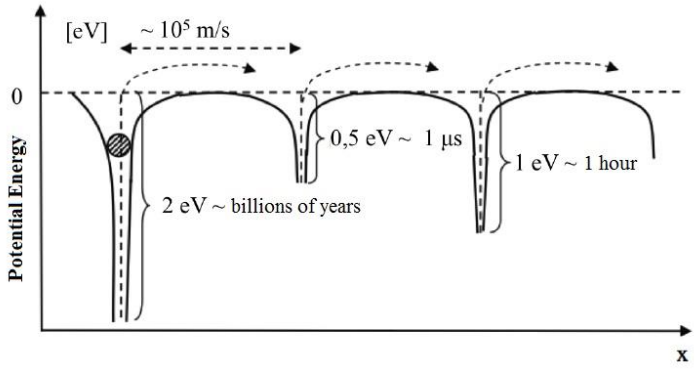

Figure 6: Charge transport through thermally activated hopping

Alternatively, electrons/holes can travel from one trap to the next via so-called quantum mechanical tunnelling. If a charge is freed from a trap, it will be attracted by the next one. As can be induced from *Figure 5*, electrons usually spend more time in traps than they do travelling between them. For traps with a depth of less than 0.5eV, the trapping time at 20°C can be shorter than 1μs, while for traps deeper than 1eV it can last for several hours [7]. Considering that electrons have an average speed of 10^5 m/s, it is no wonder they usually spend more time in the traps.

2.5.4. Charge injection from the Electrodes

Injection of electrons at the cathode and extraction at the anode is the main mechanism for transport of charge in polyethylene. Injection of charge is often discussed in terms of *Fowler-Nordheim injection* and *Schottky injection*. Also in the case of an electron crossing the boundary between the electrodes and the insulation, there is a potential energy barrier the electron needs energy in order to pass. The magnitude of this barrier depends on the interface between the electrode and the insulation, and their respective materials.

The energy needed for an electron to cross the potential energy barrier is given by the equation:

$$W = \phi - \chi \tag{10}$$

Here, ϕ is the work function of the metal, and χ is the electron affinity. An illustration of their relationship and the potential barrier can be seen in *Figure 6*. ϕ represents the barrier, while χ is the materials ability to receive electrons and form negative ions.

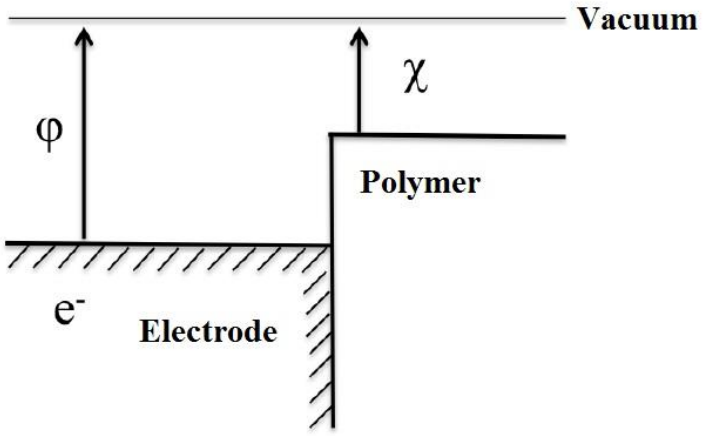

Figure 7: Potential barrier of the electrode-polymer interface [3]

Reminiscent of the *Poole-Frenkel mechanism*, *Schottky injection* is injection of charge aided by a reduction of the height of the potential barrier due to an increase in field intensity. An increase in field and/or temperature reduces the height and width of the potential barrier, and thus increases the probability that there will be electrons with sufficient energy to cross the barrier. With *Schottky injection*, the current density is given by Equation 10 and is dependent on the temperature T and electrical field E [3]:

$$J = AT^2 e^{\left(\frac{\phi - \sqrt{\frac{e^3 E}{4\pi\epsilon_0\epsilon_r}}}{kT}\right)} \tag{10}$$

Here, A is Richardson's constant, T is the temperature, and ϕ is the total height of the potential barrier. This equation is relatively accurate for fields up to 100kV/mm.

For fields higher than 100kV/mm, a quantum-mechanical process called *Fowler-Nordheim injection* is possible. With a strong applied field, if the width of the potential barrier is sufficiently diminished, it makes the transport of electrons through a tunnelling mechanism possible. This can lead to electrons crossing the potential barrier even without sufficient energy. In this case, the current density depends little on the temperature, instead varying greatly with the electrical field:

$$J = BE^2 e^{\left(\frac{-C\varphi^{\frac{2}{3}}}{E}\right)} \tag{10}$$

Here, B and C are constants, and $\varphi = \phi - E_{fermi}$.

These two processes mirror the two ways mentioned for charge transport between traps. In practice, the potential barrier is difficult to predict, as it varies greatly depending on factors such as electrode material, pressure in the interface, chemical and electrical defects such as surface roughness, moisture and other impurities, local polarisation and more [3,8,9].

2.5.5. Classification by Charge Position

Accumulations of space charges are usually classified as homo- or hetero charges, depending on whether they have the same charge as the adjacent or opposite electrode, respectively [8].

Homo Charges

Generally, charges injected by the electrodes are responsible for homo charge in the material. In this case, the transportation of charge in the material is slower than the injection, causing a build-up of charge in the vicinity of the injecting electrode [1]. Homo charges will generally cause a reduction of the field close to the electrodes, while the field in the bulk of the insulation is increased [1].

Hetero Charges

Homo charge can be generated by ionisation of dissociable chemical species present in the polymer. An applied field will cause electrons and positive ions to travel towards the electrode of opposite polarity, where they can be trapped. In this case, charge transport prevails over injection, causing hetero charges [1]. Hetero charges can also accumulate due to one of the electrodes blocking the extraction of free charges injected by the other electrode. Contrary to homo charges, hetero charges lead to increased field stress close to the electrodes, and decreased stress in the bulk of the insulation [1].

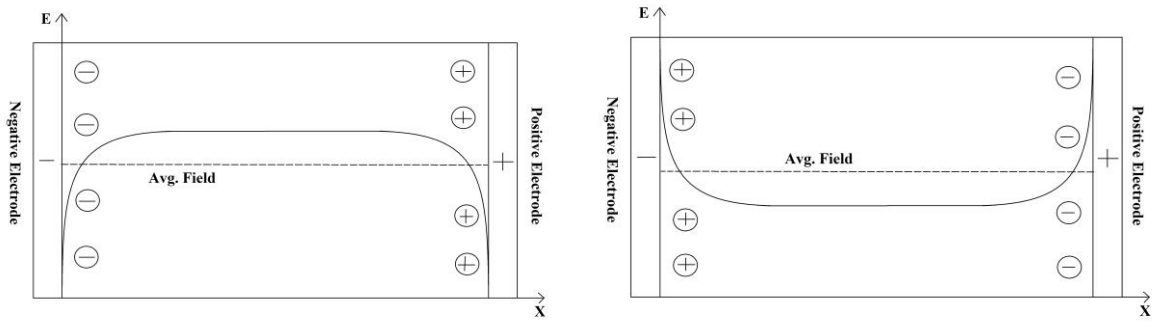

Figure 8: Homo and hetero charge with field influence

Changes in the field distribution in cable insulation caused by space charges can lead to areas with increased stress, which in the worst case scenario can exceed the break

down strength of the material and lead to failure. Increased stress can also lead to formation of weak points in the insulation, causing an acceleration of the ageing process of the material.

Following a change in polarity, hetero and homo charges will switch, turning areas with decreased field stress into areas with increased stress. When charge transport prevails, the charge will also cross the material rather quickly, leading not only to recombination, but also possible damage to the structure of the material [1].

2.5.6. Polarisation

Electronic

Electronic polarisation occurs when an atom is positioned in an electrical field. The field causes the negative electron cloud to distort in one direction and pushes the positive nucleus in the opposite direction, causing a temporary dipole moment proportional to the field. The polarisation is instantaneous and will disappear when the field is removed [4].

Ionic

When a material has an ionic structure, consisting of cations and anions, ionic polarisation is possible. Anions and cations held together by an ionic bond possess a dipole moment before a field is applied, but the total sum of dipole moments in the whole material may still be zero. When a field is applied, the anions and cations are pushed in opposite directions by the electric field, distorting the bonds so that the centres of positive and negative charge no longer coincide, and a net polarisation develops. Ionic polarisation as well is instantaneous, and will disappear once the field is no longer present [4].

Orientational

In certain materials, the molecules possess a permanent dipole. In the absence of an electric field, the dipoles are randomly arranged and will thus cancel each other out so the net polarisation is zero. When an electric field is applied, the dipoles will orient themselves to align with the field, and a net polarisation occurs. In gases and liquids, the dipoles are free, and the polarisation P_d is approximately proportional to the field. In solids, the relation between the applied field, temperature, and polarisation must be determined experimentally. Orientational polarisation is characterised as a relaxation mechanism, and will not disappear instantaneously when the field is removed [4].

Interface Polarisation

Maxwell-Wagner (MW) polarisation can be used to describe the accumulation of charge in interfaces. According to MW, space charge will accumulate in the interface

if the ratio between the conductivity and permittivity of the materials of the interface differ [10].

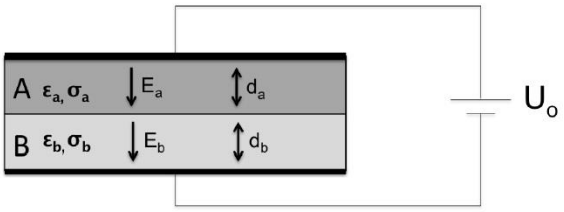

Figure 9: Layered insulation with different conductivity and permittivity [10]

When a voltage U_0 is applied, the accumulation of space charges in an interface can be described by the following equation:

$$\kappa(t) = \frac{\epsilon_A \sigma_B - \epsilon_B \sigma_A}{d_B \sigma_A - d_A \sigma_B} U_0 \left(1 - e^{\left(-\frac{t}{\tau_{MW}}\right)}\right) \tag{11}$$

Where $\kappa(t)$ is the time dependent space charge in the interface, d_A and d_B are the thickness of the layers, σ_A and σ_B are the conductivity, and ϵ_A and ϵ_B are the permittivity of the two materials. The time constant is given by the equation:

$$\tau_{MW} = \frac{\epsilon_B d_A - \epsilon_A d_B}{d_A \sigma_B - d_B \sigma_A} \tag{11}$$

2.6. Detection of Space Charges

2.6.1. Pulsed Electro-Acoustic Method (PEA)

In order to detect space charges, the method used in the work presented in this thesis is the pulsed electro-acoustic method. This method is the most widely used because of its simplicity and low costs [11].

The principle behind the method can be understood through *Figure 10*. A dielectric material of thickness d is placed between two electrodes, and a DC voltage V_{dc} is applied. Consequently, a space charge $\rho(x)$ will accumulate in the material as time progresses. The space charges are detected using an electric pulse, $V_p(t)$, which induces a force acting on the charges, causing them to move in accordance with the pulse. These movements generate an acoustic wave propagating in the material, which is subsequently detected by a piezoelectric transducer and converted into a time dependent electrical signal, V(s):

$$V(s) = K[\sigma_1 + \sigma_2 + v_{sa}\Delta T\rho(x = v_{sa}t)]e_p \quad (11)$$

Where σ_1 and σ_2 are the charges on the electrodes, v_{sa} is the sonic speed in the material, ΔT is the duration of the pulse, ρ is the charge, e_p is the amplitude of the pulse, and K is the calibration constant.

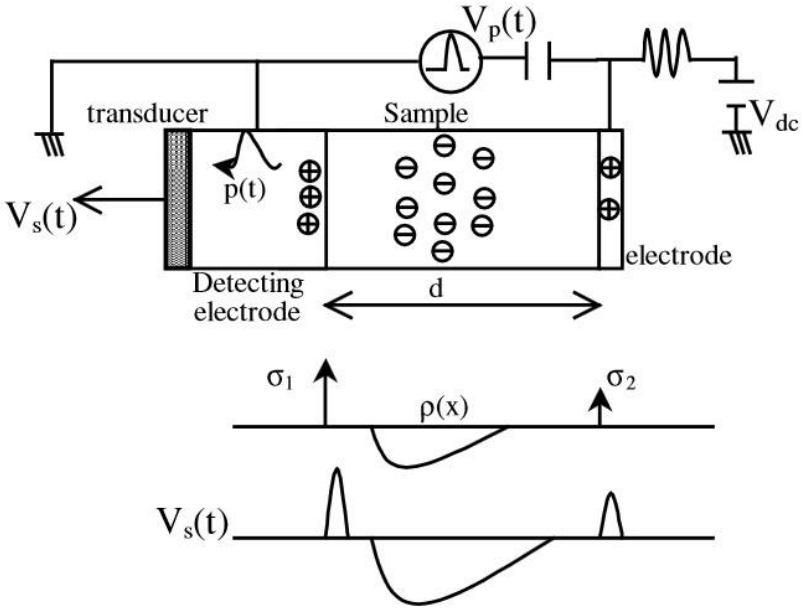

Figure 10: Schematic of the PEA system [11]

2.6.2. Calibration

Because of attenuation and dispersion, the signal received by the transducer will not directly correspond to the charges in the material. The amplitude of the pressure wave caused by the charges is reduced as it travels through the material. This dampening of the signal is frequency dependent, and higher frequencies will be more attenuated compared to lower frequencies. Attenuation is mainly caused by the absorption and dissipation of the acoustic energy into heat or other forms of energy, while dispersion may be caused by the scattering of the acoustic waves due to densely distributed inhomogeneities and frequency dependence of material constants. [12]. Compared to signals obtained in an ideal test object without acoustic impedance, the amplitudes of the signal will be smaller, and the width larger. This effect is amplified with the distance travelled by the acoustic waves in the material. An illustration of this principle is shown below:

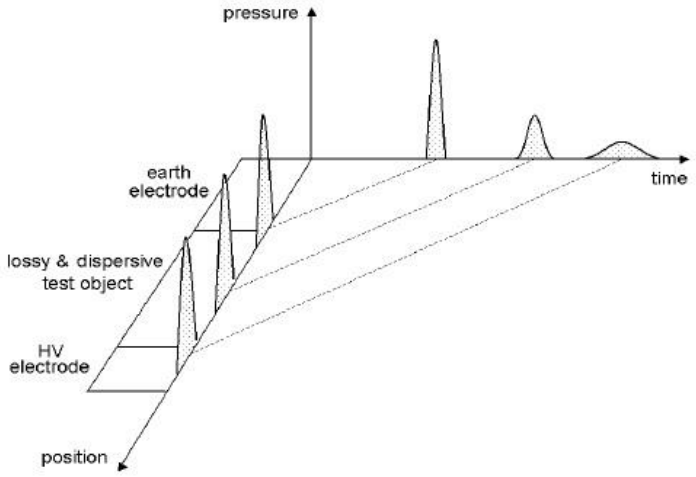

Figure 11: Attenuation and disperion of acoustic waves in the PEA method [13]

For this reason, a calibration of the equipment is necessary before the actual experiment can be effected. Since there are variations between samples even if they are made of the same material using the same process, calibration is necessary before measurements are done with a new sample.

2.7. Measuring Degree of Crystallinity

Additional energy is released when melting semicrystalline polymer. The energy released during the melting of a material sample can be measured using differential scanning calorimetry (DSC). DSC measures the amount of heat required to increase the temperature of a sample, as well as a reference with a well-defined heat capacity. When the sample undergoes physical transformations, it will require more or less heat than the reference in order to keep them at the same temperature. The difference in heat flow between the sample and the reference observed by the calorimeter allows it to measure the sample's energy released or absorbed, in other words its change in enthalpy, ΔH. It is then possible to calculate the crystallinity of the sample through comparison with the energy released when melting a standard sample of the same material with a known degree of crystallity.

2.8. Detrimental Effects of Space Charge

A link between space charge accumulation and ageing of insulation material has been proven [1]. Accumulated charge can drastically alter the poissonian field, store electromechanical energy, and cause radiative recombination-excitation. These processes can cause damage through increased rate of generation of hot electrons, reduction of the energy barrier of degradation reactions leading to bond dissociation, microcavity enlargement and internal strains [3].

In some cases, the field may even be deformed to such an extent that it exceeds the breakdown strength of the dielectric, causing failure. But even if the field does not exceed the breakdown strength, local weak points can be formed through the processes mentioned, accelerating the ageing of the material. It has been shown that a field increase of 50% means about a 60 times life reduction, considering an inverse-power life model with a voltage endurance coefficient (VEC) of 10 [14].

Space charge is also an effect of aged material, as ageing can modify the chemical-physical properties of the material, the trap level distribution, and thus also the charge injection effectiveness [15]. It has been shown that for the same material under identical condition, specimens where space charge accumulates faster consistently develop breakdown faster than in specimens where the development of space charge is slower [4].

Chapter 3

Methodology
This section contains a description of the process of producing samples, and the practical steps of setting up the measurements with the PEA equipment.

3.1. Production of Flat, Layered Samples

The flat samples consist of two layers of HVDC material (LE4253DC15), one cross-linked only once, and the other cross-linked twice. The material is delivered from the manufacturer in the form of pellets, which are then extruded into a more manageable thin film. The first layer is made from pieces of the thin film, which are press-moulded and cross-linked in a hydraulic press, and then thermally pre-treated for three days. The second layer is moulded without being cross-linked, and then the two layers are cross-linked together in the press, before being pre-treated for three new days. Finally, gold electrodes are added on each side of the samples using an ion sputter. These steps will be explained in closer detail later.

Cleanliness is essential throughout the production, as even the smallest amount of contamination can have an influence on the accumulation of charge in the material. All tools used are therefore thoroughly cleansed with isopropanol in a laminar flow cabinet, and all of the processes are performed in close to sterile conditions in the lab.

3.1.1. Extrusion

The insulation material is stored as pellets, which are then extruded into a sheet of the desired thickness, in order to avoid voids and to reduce pollution in the material.

The principle of the extruder is shown in *Figure 12.* Pellets are fed to the extruder through the hopper. Next, the material is transported by a rotating screw while being heated by the heaters and the mechanical work exerted on the material by the screw. As the material gets closer to the head of the extruder, the distance between the threads of the screw is gradually reduced, causing increased pressure and a reduction of voids in the material. At the mouth of the extruder head, the material is shaped into the desired thickness. A photograph of the extruder, along with some other clarifying pictures is shown in [A.IV.a].

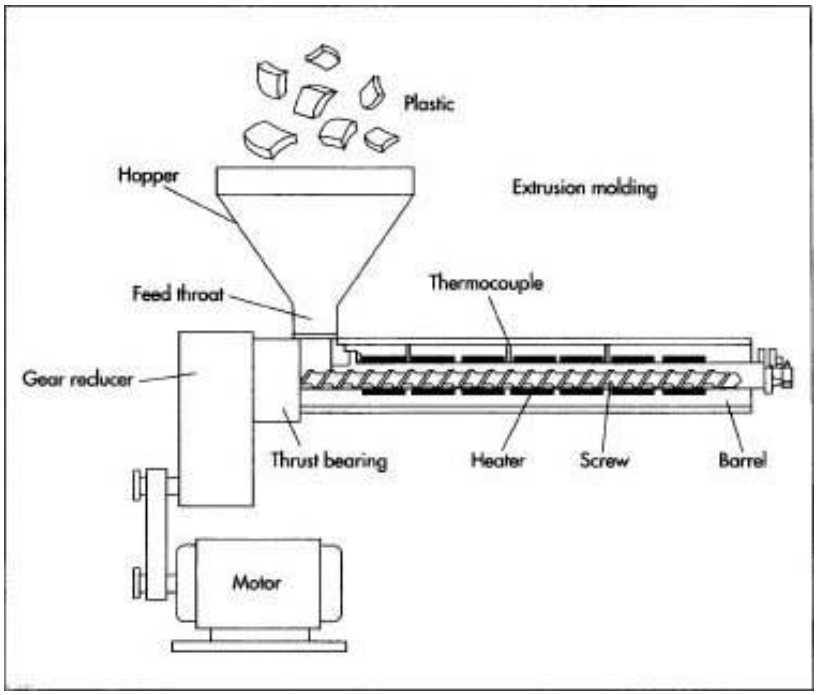

Figure 12: Plastic Extruder Schematic

The extruder is divided into six temperature zones, and the settings used for each zone can be seen in *Table 1*. Before starting the process, the extruder is disassembled and all the individual parts are thoroughly cleansed using isopropanol. The extruder is then pre heated for about an hour so that all the zones have an even temperature. During the extrusion, the rotating screw is set to rotate at 14 rpm, resulting in a pressure at the head of around 140 bar.

Zone	Temperature [°C]
1	117
2	117
3	117
4	117
5	117
6	17

Table 1: Temperature settings for extruder zones

After the material has exited the extruder head in the form of a thin film, the film is cooled and its shape is maintained as it is rolled through a water cooled drum. After cooling, the thin film is finally rolled onto a rotating drum. The first meter of material to exit the extruder is discarded because of impurities that may arise in the beginning of the extrusion process.

After use, pellets of a softer material are run through the extruder on the same program as the one used to extrude the insulation material. The material of the rinsing pellets is softer, and thus easier to remove after the machine has cooled down.

This makes it significantly easier to clean the extruder. Finally, the parts of the machine which have been in contact with the material are cleansed with isopropanol and copper brushes.

3.1.2. Moulding and Cross-linking

The finished plastic film is cut into pieces of approximately the same size, with a total weight of 2,8g. These pieces are placed in moulds with a diameter of 7,5cm, and shims with a thickness of 1,75mm are used in order to achieve a thickness of 0,25mm for the test objects.

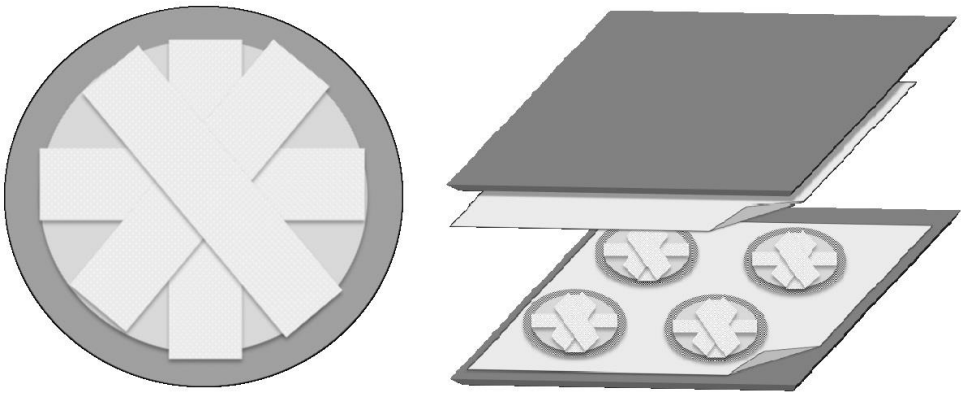

Figure 13: Polymer film in press mould and moulds between metal plates [2]

The moulds are placed between two metal plates, with a sheet of plastic acting as a barrier between the metal and the test objects in order to avoid contamination and physical damage.

The hydraulic press is pre-heated to 120°C before the moulds are inserted. The program run in order to form and crosslink the samples is shown in *Table 2* and *3.*

Setting	Pressure [Tons]	Temperature [°C]	Time [Minutes]
Low Pressure	3.5	120	10
High Pressure	25	120	2
Water Cooling	25	-	12

Table 2: Program for press-moulding samples without cross-linking

Setting	Pressure [Tons]	Temperature [°C]	Time [Minutes]
Low Pressure	3.5	120	10
High Pressure	25	170	40
Water Cooling	25	-	18

Table 3: Program for cross-linking samples

Photographs of moulds and the hydraulic press are shown in [A.IV.b].

3.1.3. Cross-linking

The first layer of material is first moulded by running the program shown in *Table 2*, and then cross linked by the process presented in *Table 3*. This layer is then thermally pre-treated for three days in a heating cabinet at 90°C and atmospheric pressure. This reduces undesired remnants of gases and anti-oxidants in the material, which could later cause accumulation of space charge.

The second layer is moulded in the same manner using only the first program *Table 2,* before the two layers are cross linked together as shown in *Table 3.* This time, the shims used are 1,55mm in order to accommodate double layers. At last, the samples with one cross linked and one double cross linked layer are placed in the heating cabinet for three days.

One sample consisting of only one layer of cross-linked material was also produced, using the same procedure as the first layer of the layered samples, only with thinner shims, so that the sample would have the same thickness as the layered samples.

3.1.4. Ion Sputtering

The last step of the production is applying the gold electrodes to the samples using an ion sputter. First, the object is placed between two plastic clamps, with a hole in the middle of each where the gold is going to be applied. The plastic clamp with the sample inside is then placed in the vacuum chamber of the sputter, the machine is turned on, and the vacuum is allowed to build for approximately five minutes. After this, the voltage is turned on at 1200V, and the vacuum adjusted until a current of 5mA is observed. The voltage and current are on for 5 minutes, before the machine is turned off, the sample flipped, and the process repeated on the other side of the sample.

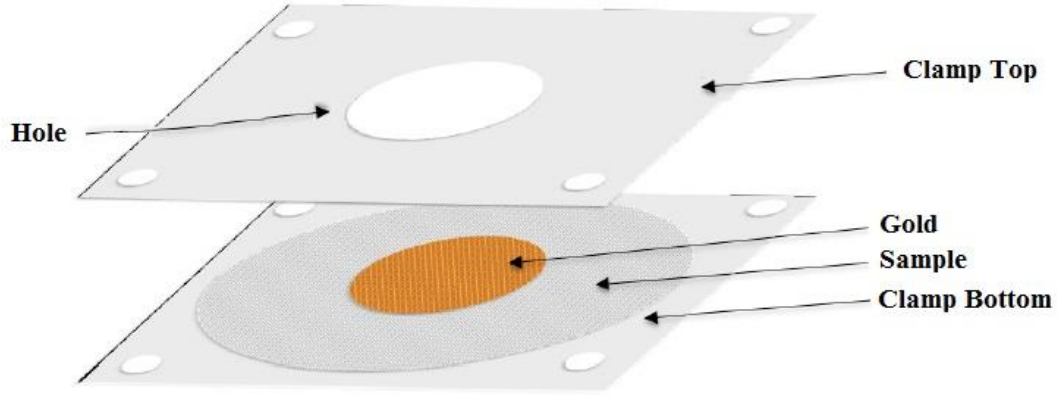

Figure 14: Clamps for ion sputtering and sample [2]

3.2. Measurement Methodology

3.2.1. Space Charge Detection

The measuring equipment used in the work presented in this thesis is a *TechImp Pulsed Electro-acoustic* (PEA). In [A.IV.c] photographs of the PEA system can be seen. The theoretical basis on which this equipment works is described in closer detail in Section 2.5. This equipment must be calibrated as described in Section 2.6.2 before the series of space charge measurements is started. The equipment has a sensitivity of $0{,}1C/m^3$, and is controlled through LabVIEW, a program which adjusts the voltage and performs measurements according to the user's input. The values obtained by LabVIEW are processed in MATLAB.

The configuration of the equipment used, a piezo-electric measurement unit and a pulse generator, is shown in a schematic in *Figure 15*. A pulse of 500V with a pulse length of 10nm and a frequency of 150Hz is generated by the pulse generator. The measurement unit is placed inside of a faraday cage, and consists of a lower aluminium electrode (cathode), and a semi-conductor connected to a brass electrode (anode) [17].

Before the sample was placed in the measurement cell, the inside of the cell is cleansed with isopropanol, and a thin film of silicon oil is applied to the centre of the aluminium electrode, as well as on each side of the semi-conducting material which is in contact with the brass electrode. This oil ensures proper acoustic contact between the sample and the electrodes.

With the test sample inside of the cell, the upper electrode is fastened with a torque wrench set to 25Nm. The equipment is connected to an oscilloscope, a computer, and a DC voltage source capable of delivering a voltage of 0 – 30kV.

During the work presented here, space charge measurements have been performed on five samples. First, measurements were done on layered test objects, consisting of two layers of the same material, but with one layer cross-linked once, and the other twice. Voltages of 20, 30 and 40kV were applied on three corresponding test objects, for 19 days, with measurements being taken at intervals as shown in [A.III]. At each specified time, 10 measurements were done with the voltage on, before the voltage was turned off, and 20 new measurements were done after a delay of one minute.

After measurement series had been run on the three layered samples, a sample consisting of a single cross-linked layer was placed in the measurement cell, and a voltage of 15kV was applied. This was done to provide results to compare with the measurements from the layered test objects, and to see if there were any significant differences depending on the interface in the material. A voltage of 15kV was chosen because the results from the measurements on the layered test object under 15kV was the clearest (more space charges than 10kV, and less noise than 20kV), and therefore easiest to use for comparisons. After this, measurements were done on a fourth layered sample with a voltage of 15kV, in order to provide further basis for reference.

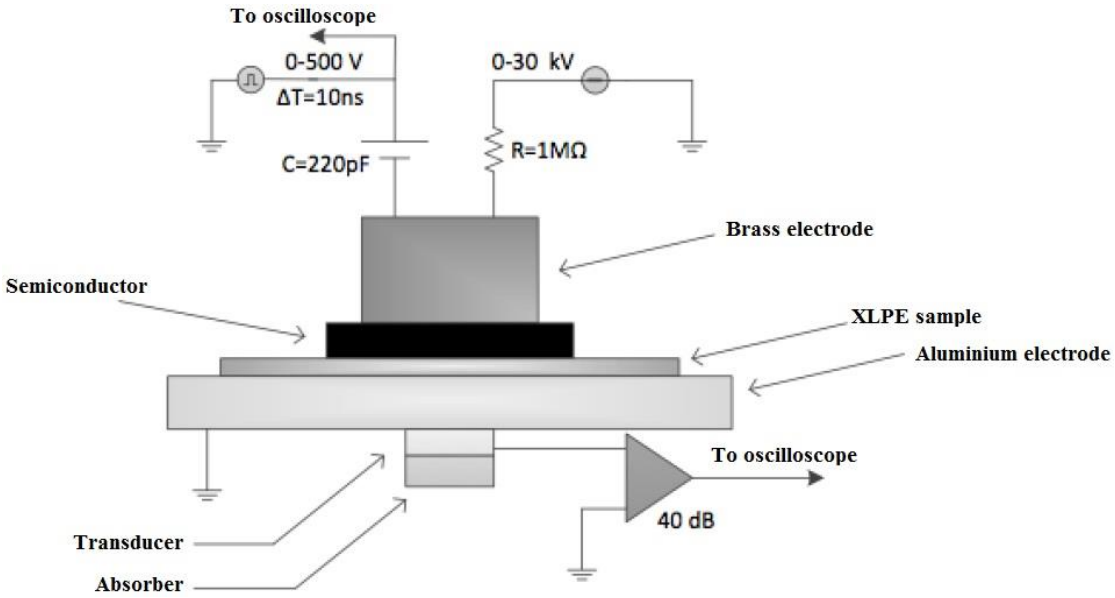

Figure 15: TechImp PEA measurement system [17]

3.2.2. Measuring the Degree of Crystallinity

In order to decide whether a difference in the conductivity of simply cross-linked and double cross-linked material could be a cause of space charge accumulation, the degree of crystallinity was measured for two specimens. One was a combination of simply cross-linked material and double cross-linked, while the other was only simply cross-linked. By comparing the (average) degree of crystallinity of these two specimens, the possible difference in conductivity could be examined.

The specimens were taken from material left over in the production of the flat test objects, so that any difference in the degree of crystallinity would be in accordance with a difference in the test objects. The reason specimens were not made from each of the two layers of the same specimen is that it would be too difficult to separate the layers once they have been cross-linked together. By measuring the difference between layered and unlayered specimens, one can get a good indication of whether the second crosslinking influences the crystallinity of the material, which in turn influences its conductivity.

The specimens were placed one after the other in a high pressure differential scanning calorimetry machine by Mettler Toledo, where a heating process was run. The melting curves of the material were detailed in Mettler's STARe software, were the crystallinity of the materials also could be calculated. In order for the software to calculate the crystallinity of the materials, their ΔH_c value (the melting point of the material in 100% crystalline form) was needed as input. For polyethylene, this has been determined to 277 J/g [18]. The beginning and end of the materials' melting curves also had to be manually marked on the curves.

Two processes were run on specimens of each type (in total four specimens). One quick and one slow heating process were run so that the results would be more precise. With a slower heating of the specimen, crystallisation may occur during the melting, thus interfering with the results. A quicker heating of the specimens will avoid this problem, but because the process is faster, it is preferential to start at a lower temperature so the sample stabilises before it reaches the interesting areas. Since the equipment used here was unable to start at a lower temperature than 25°C, this could be a source for error. Both a slow and a quick heating process were run in order to obtain increased confidence in the results.

Chapter 4

Results

In this chapter, the results of the measurements done will be presented, while the interpretation of these results will be left for chapter 5.

4.1. Sample 1

4.1.1. Space charge distribution

Voltage On

The space charge distribution in the sample with an applied voltage of 10kV is shown in *Figure 16.* Accumulation of charge is at first only visible at the electrodes, and the maximum and minimum of the charge continue to stay there, although some changes are apparent. At the cathode, the charge reaches its maximum quickly, reaching -11.27C/m3 after 10 minutes. After this, the charge density gradually diminishes throughout the rest of the time period, ending at -5.79C/m^3 after 19 days.

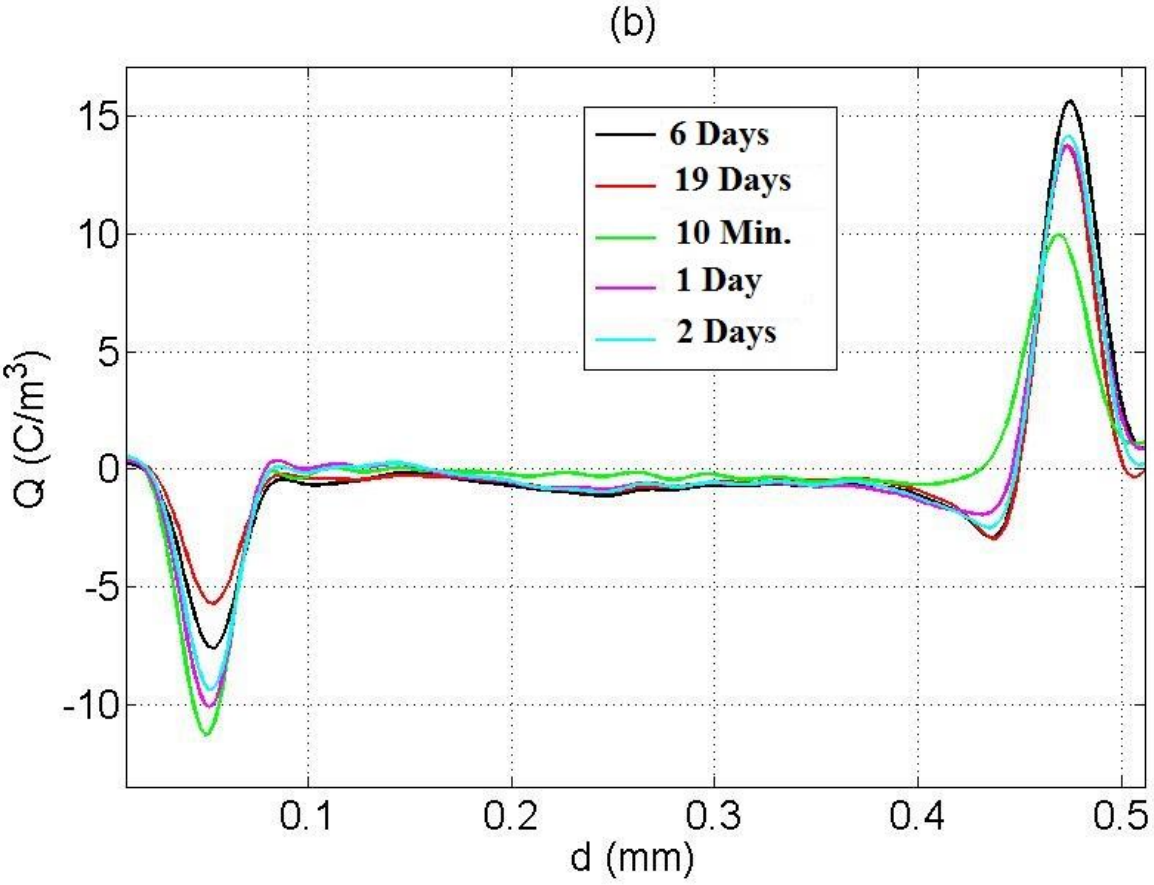

Figure 16: Space Charge Distribution Sample 1, Von

At the anode, amount of charge increases quickly the first 10 minutes, reaching 9.93C/m^3. The rate slows down, but continues to be quite fast the first 24 hours, reaching 13.73C/m^3. A maximum of 15.62C/m^3 is reached after 6 days, when the development turns negative. At the final measurement, the density has decreased to 13.73C/m^3. There is also a local minimum in the bulk towards the anode appearing after the first two days. After this, the development slows down, and after 5 days, the accumulation stabilises at around -3C/m^3, with little change towards the end of the measurements.

The development in the bulk of the material looks noisy, but a local negative maximum appears to develop at around 0.25mm during the first 5 hours (the maximum drifts from 0.21mm towards 0.25mm), reaching a maximum of -1.1C/mm^3 by the end of the measurements.

There is some hetero charge close to the cathode after 24 hours, but as more negative charge accumulates in the bulk, the net charge of this area also turns negative.

Voltage Off

The charge density distribution with the voltage turned off is shown in *Figure 17*. The same development can be seen here as with the voltage on, with the charge density at both the cathode and anode having a positive difference from the first measurements to the last.

In the first measurements, after 10 minutes, there is a slight amount of homo charge at both electrodes, but this turns into hetero charges at the cathode during the first 120 minutes as positive charge accumulates. The now positive charge at the cathode continues to grow denser, reaching a maximum of 3.40C/m^3 after 8 days. After this the density diminishes slowly towards the last measurement, ending at 2.90C/mm^3.

The charge accumulation at the anode reaches its maximum of 9.89C/m^3 after 15 days, before ending at 9.16C/m^3 at the last measurement. The accumulation of negative charge in the bulk, close to the anode, follows the same pattern as with the voltage on, although reaching a slightly larger negative value of -3.573C/m^3.

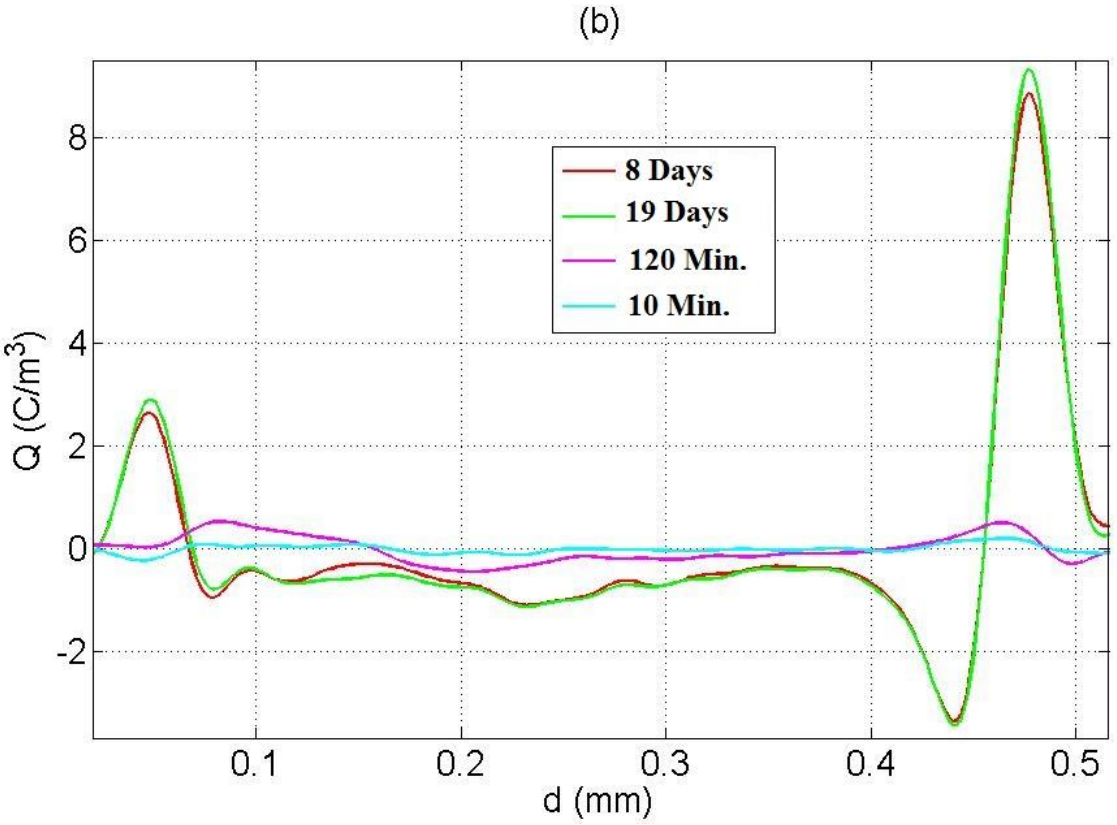

Figure 17: Space Charge Distribution Sample 1, Voff

The charge density in the central bulk of the material is about the same as with the voltage on, with a slightly larger negative value of -1.15C/m^3.

4.1.2. Field Distribution

A voltage of 10kV was applied to the first sample. Since the thickness of the sample was 0.4163mm, the average field in the sample should have been approximately 24kV/mm. As can be seen from *Figure 18*, the field after 5 minutes with the voltage on is measured to be around 17kV/mm, with a lower field closer to the cathode, and a higher field closer to the anode. The field distributions calculated using the measurements tend to contain quite a bit of error when it comes to absolute values, and as such, the focus will be more on the shape of the field distributions.

In the first measurements, the field strength in the bulk at the anode side is increased as negative charge accumulates. This also leads to a lower field at the cathode side, and the shape of the field distribution changes little after the first 24 hours. The homo charge at the electrodes greatly diminishes the field at the ends of the curve, and should increase the field in the entirety of the bulk. This, however, is difficult to see, since the absolute values cannot be trusted.

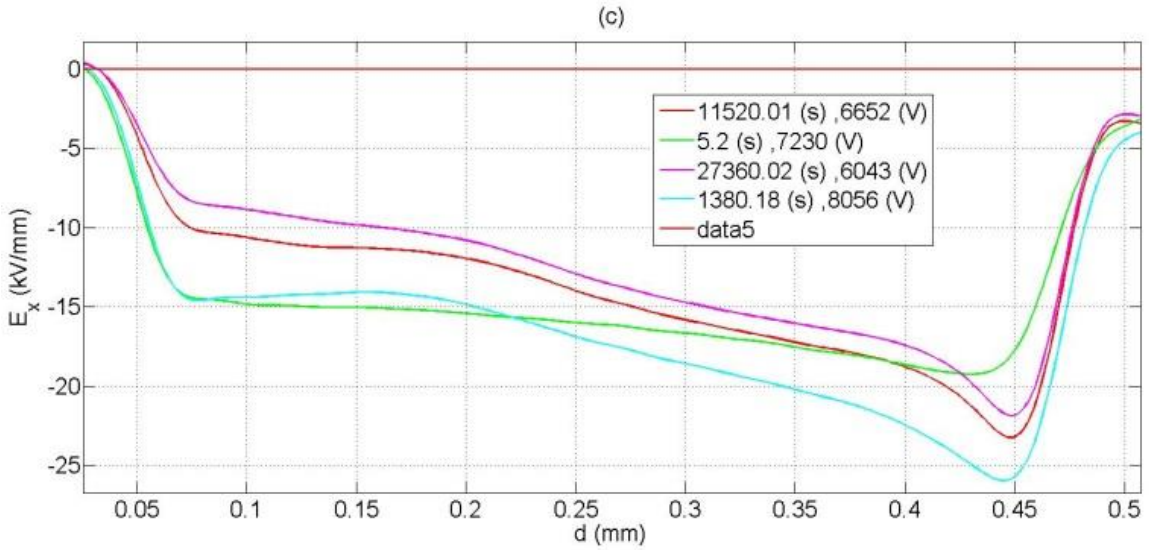

Figure 18: Field Distribution Sample 1, Von

Looking at *Figure 19*, the field in the sample with the voltage turned off, the field contribution due to space charge can be seen.

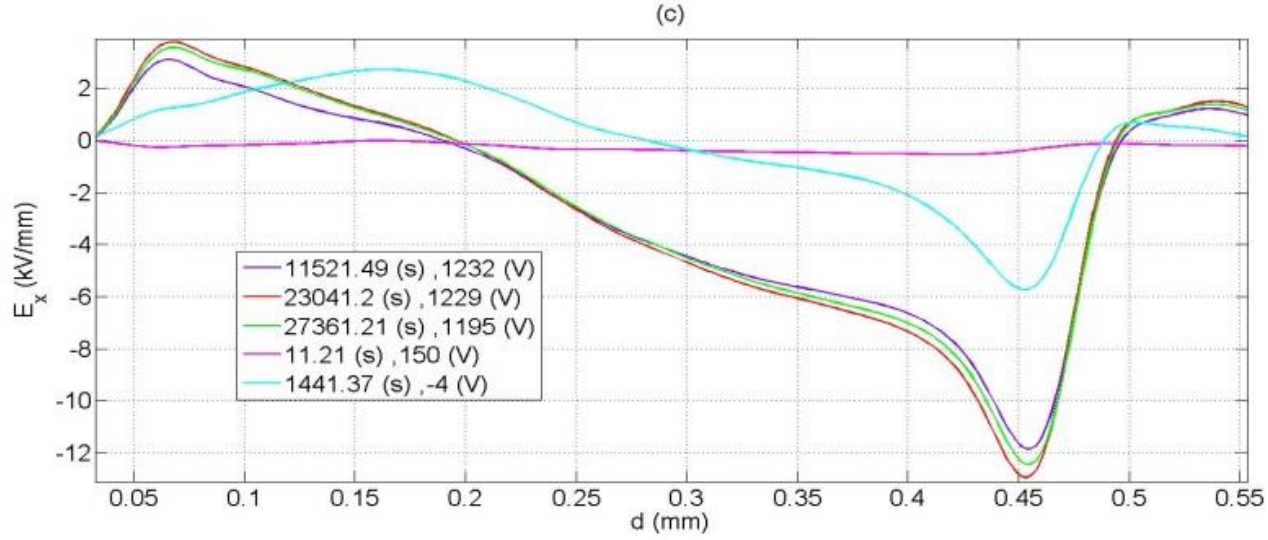

Figure 19: Field Distribution Sample 1, Voff

There is only a slight contribution during the first measurement, with some positive field contribution at the cathode side, and a small negative contribution on the anode side of the material – leading to the slight angle observed in the first voltage on measurement. This trend is only accentuated as time passes, with the shape changing minimally from the 5th day and to the end of the measurements.

4.2. Sample 2

4.2.1. Space charge distribution

Voltage on

A voltage of 15kV was applied to the second sample, the resulting space charge distribution of which can be seen in *Figure 20*. Here, the negative charge density at the cathode reaches a maximum of -14.64C/m^3 after 80 minutes, before it starts to diminish, finally stagnating at around 7C/m^3 after 8 days, ending at -6.57C/m^3.

The charge in the bulk by the anode reaches a maximum of -5.12C/m^3 after 12 hours, before sinking. The charge here reaches -2.99C/m^3 after 6 days, and changes little after this, ending at -2.69C/m^3. The charge at the anode also reaches its maximum after 12 hours, before sinking from 13.91C/m^3 to approximately 11.99C/m^3 by the 6th day, and ending at 11.54C/m^3.

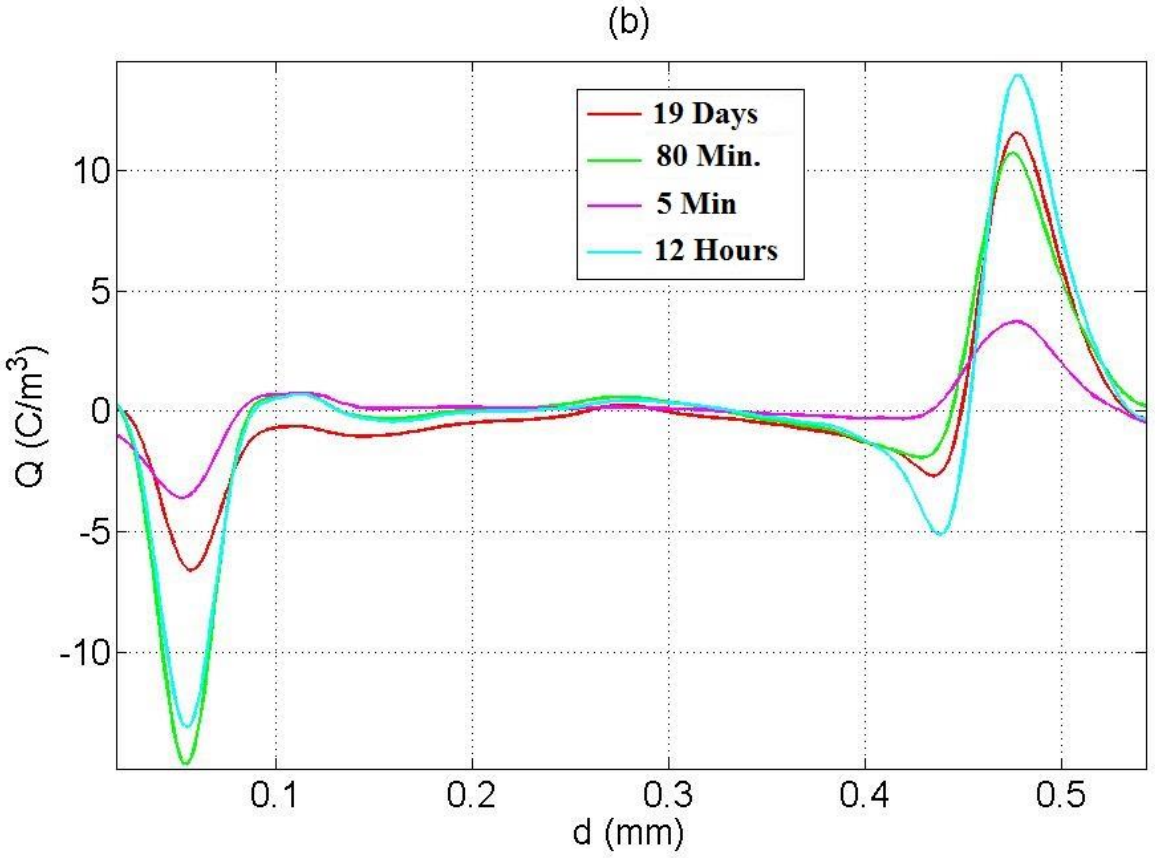

Figure 20: Space Charge Distribution Sample 2, Von

In the bulk of the material, hetero are present close to the cathode during the first 24 hours of the experiment, but as more negative charge accumulates in the bulk of the material, the net charge turns negative also here, similarly to the development observed in sample 1. There is a significant accumulation of hetero charges close to the anode as well, reaching its maximum value after 24 hours, quicker than observed in sample 1.

The point where these measurements diverge from sample 1 is on the anode side of the material interface, where the charge density stays relatively unchanged in a local, positive maximum around 0,275mm.

Voltage off

The voltage off measurements of space charge distribution in sample 2 is shown in *Figure 21*. Here as well, the reversal of the charge by the cathode is observed, as well as the increasing charge density at the anode. The homo charge at the cathode reaches its maximum of -1.96C/m^3 after 1 hour, before starting its positive development. The charge turns positive after 18 hours, slows its development after three days, at 2.79C/m^3, and ends at its maximum value of 3.73C/m^3 at the last measurement.

The hetero charge at the anode increases quickly to 4.57C/m^3 during the first 7 hours, and reaches a peak of 7.0C/m^3 after three days, before sinking down to 5.93C/m^3 by the last measurement. The hetero charge in the bulk close to the anode also builds quickly during the first 7 hours to -5.26C/m^3, reaches its peak after 24 hours at -6.57C/m^3, and ends the last measurement at -3.92C/m^3.

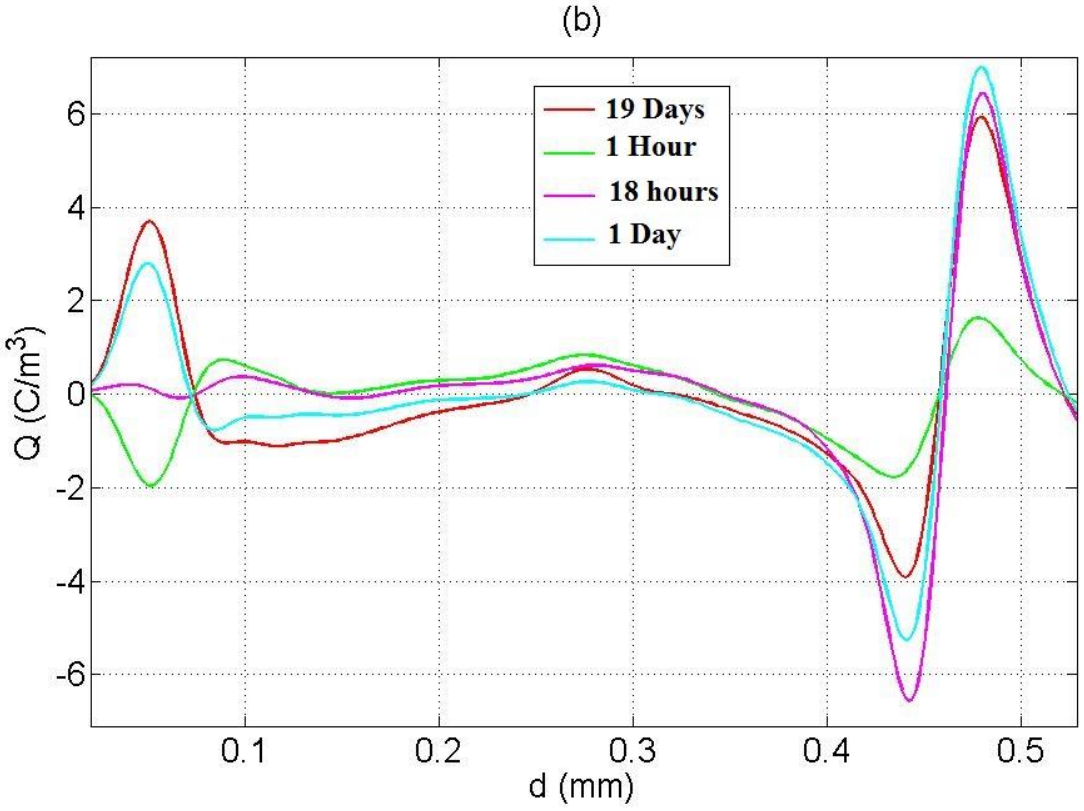

Figure 21: Space Charge Distribution Sample 2, Voff

Similarly to what was observed in sample 1, negative charge accumulates in most of the bulk of the material. The exception to this is the positive charge in the point around 0,275mm. This charge accumulation reaches a peak of 0.83C/m^3 after 1 hour.

The negative charge in the bulk close to the cathode reaches its maximum in the last measurement, at -1.10C/m^3.

4.2.2. Field Distribution

Even though the error in the field measurements is large, the influence of the charge accumulation on the shape of the field distribution can be seen. As homo charges accumulate by the cathode, the field there is weakened, while the field by the anode is strengthened by the hetero charges accumulating there. The positive charge in the central bulk leads to a steeper field on the anode side of the bulk. These trends are apparent already after 24 hours, with little change happening afterwards.

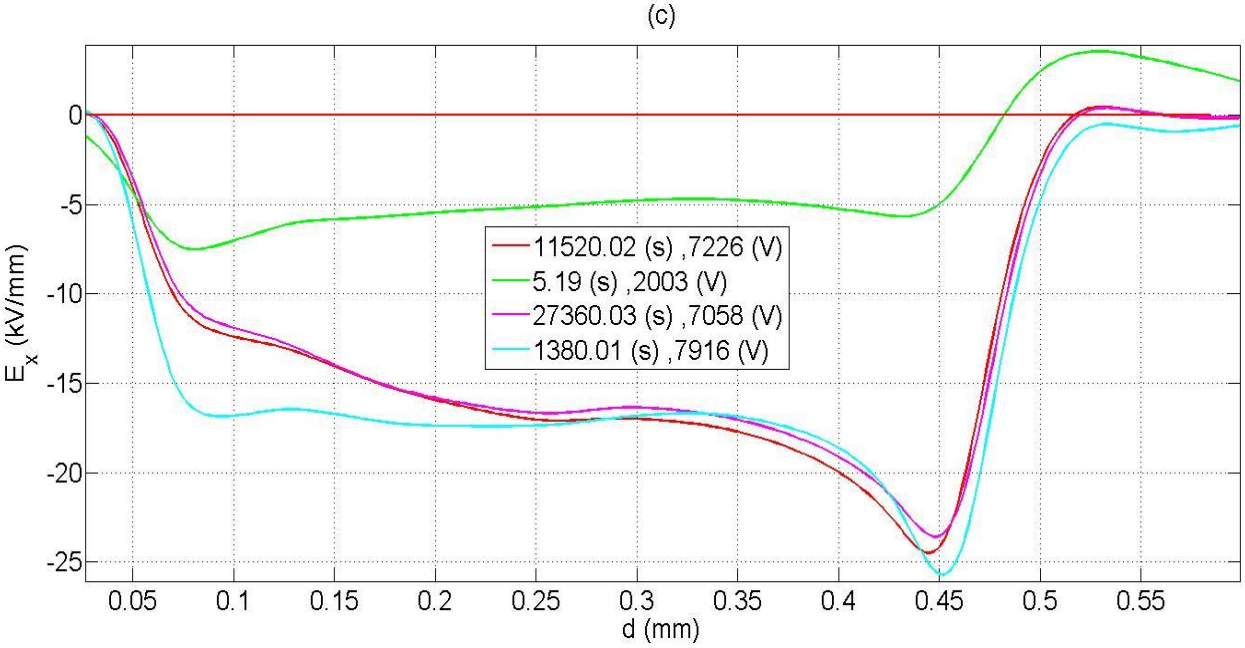

Figure 22: Field Distribution Sample 2, Von

This is reflected in the voltage off measurements, where the field is positive on the cathode side, and negative on the anode side. The apparent difference between the field curve after 24 hours and the later voltage on measurements is more pronounced with the voltage off. This also correlates with the development of the homo charges by the cathode. The warping of the field due to the positive bulk charge is also apparent here.

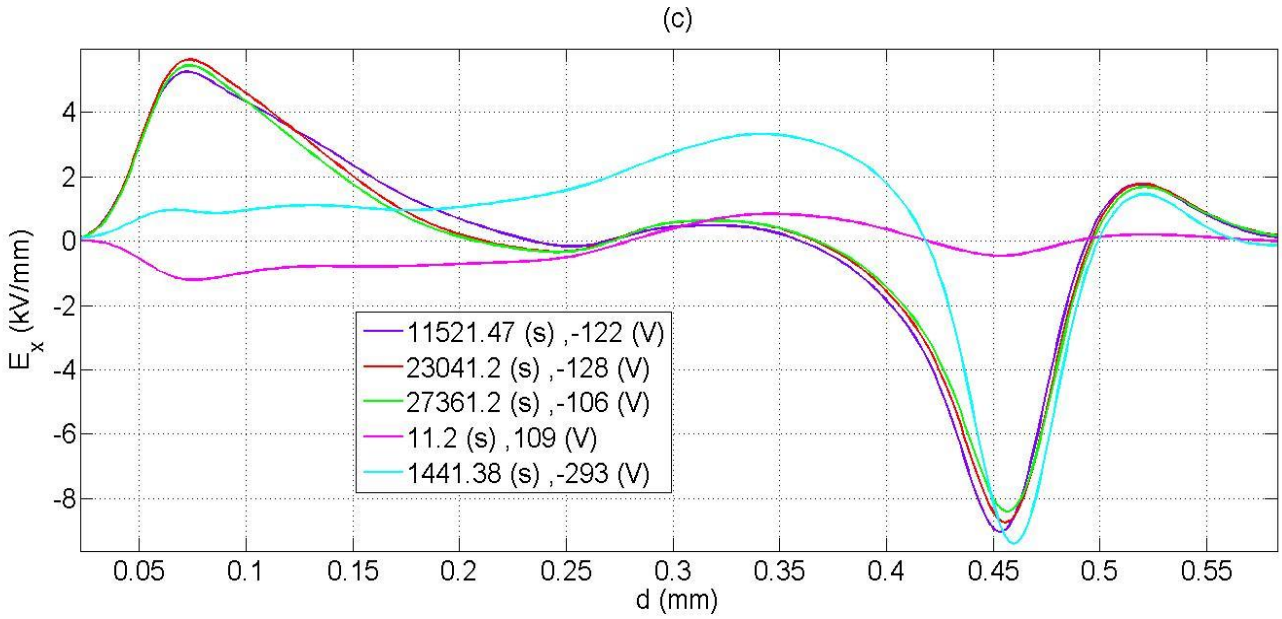

Figure 23: Field Distribution Sample 2, Voff

4.3. Sample 3

4.3.1. Space Charge Distribution

Voltage on

With an applied voltage of 20kV, the peaks at the electrodes have higher values than during the preceding tests.

The same development can be seen in as in sample 2 and 1, with the charge density at the cathode having its peak value at -24.75C/m^3 already after 5 minutes before diminishing. The charge density here diminishes quickly the first 5 hours, to --12.67C/m^3, before diminishing slower to -7.42C/m^3 after 2 days. The charge stays relatively stable after this, reaching its minimum of -6.20C/m^3 by the end of the measurements.

In the bulk by the anode, the charge reaches a peak of -13.90C/m^3 after 6 hours before sinking rapidly the next 14 hours to -4.49C/m^3. The development slows down after this, but still sinks to -2.17C/m^3 after 2 days, after which the charge stays quite stable, ending at almost the exact same value. The charge at the anode-polymer interface reaches its maximum of 56.73C/m^3 after 12 hours, before sinking, and ending at 46.99C/m^3 after some mild oscillations.

There is potentially some more noise in the signal, but throughout the measurements, there is an accumulation of hetero charge in the bulk close to the cathode. This accumulation reaches its peak of 5C/m^3 at the first measurement, and only loses

magnitude by each later measurement, most of it during the first 2 days, reaching 1.08C/m^3, and ending the last measurement at 0.68C/m^3.

There is also a local minimum at the cathode side of the material interface, reaching its largest magnitude of -3.59C/m^3 after 7 days. By the last measurement, the local minimum has a magnitude of -2.81C/m^3. At this point, the minimum has widened considerably.

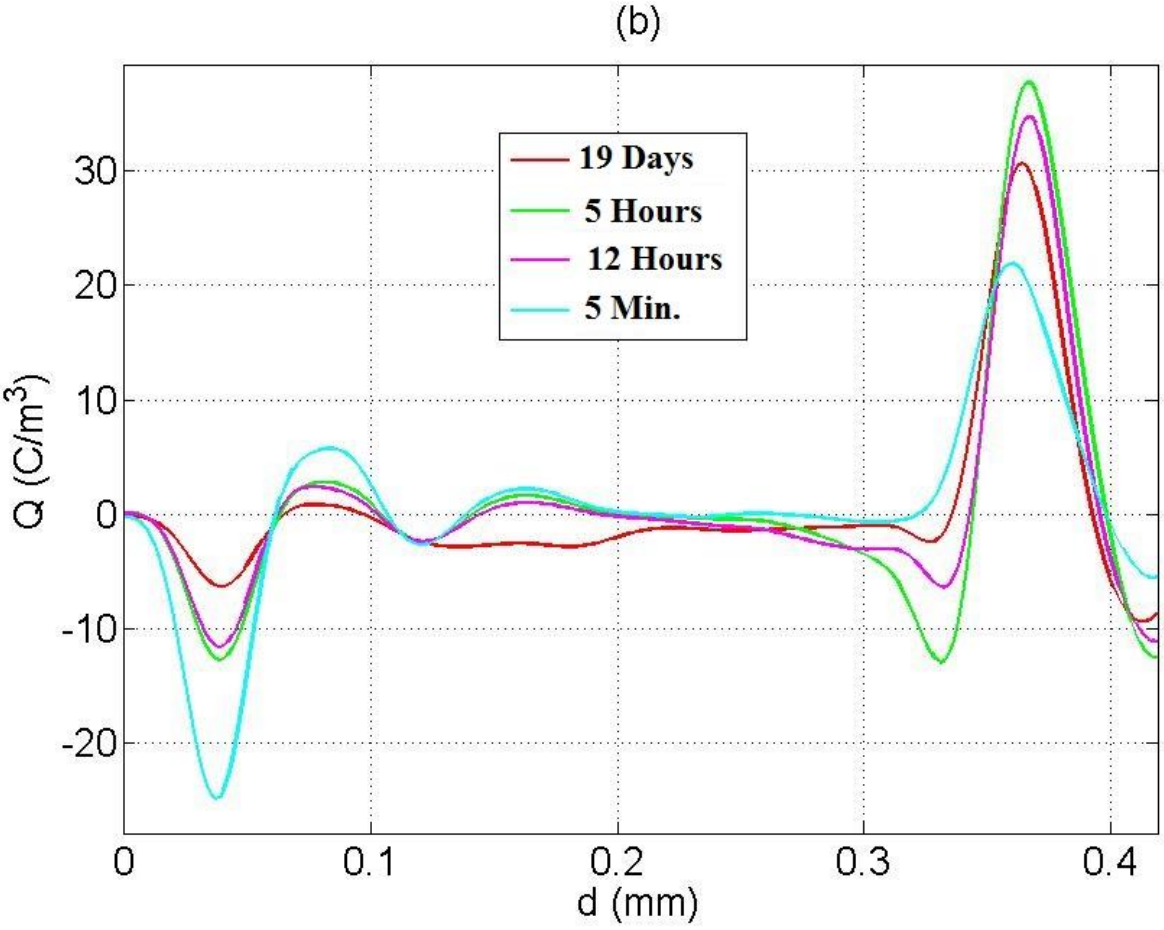

Figure 24: Space Charge Distribution Sample 3, Von

Voltage off

Excepting the charge distribution in the bulk of the material, the space charge distribution with the voltage off is as one would expect from the distribution with the voltage on, counting on the recurring trends from the previous samples. The charge at the cathode is positive from the first measurement, and there is homo charge present in the bulk by the cathode from the first measurement as well. The charge at the cathode increases quickly the first two days, up to 10.17C/m^3. The increase continues more slowly up to 11.09C/m^3 at the last measurement. The homo charge peaks after 3 days, at -4.71C/m^3.

The hetero charge in the bulk by the anode peaks at -12.17C/m^3 after 6 hours, while the charge at the anode peaks after 7 hours at 21.00C/m^3. The charge at the anode goes down to 13.14C/m^3 after 6 days, before rising up to 14.96C/m^3 in the last measurement.

The charge distribution in the central bulk of the material has some local peaks developing throughout the measurements. By the last measurement, there is are maxima at 0.132mm, 0.239mm and 0.317mm, while minima are present at 0.185mm and 0.278mm. The maximum difference in charge density between these points is 2.94C/m^3.

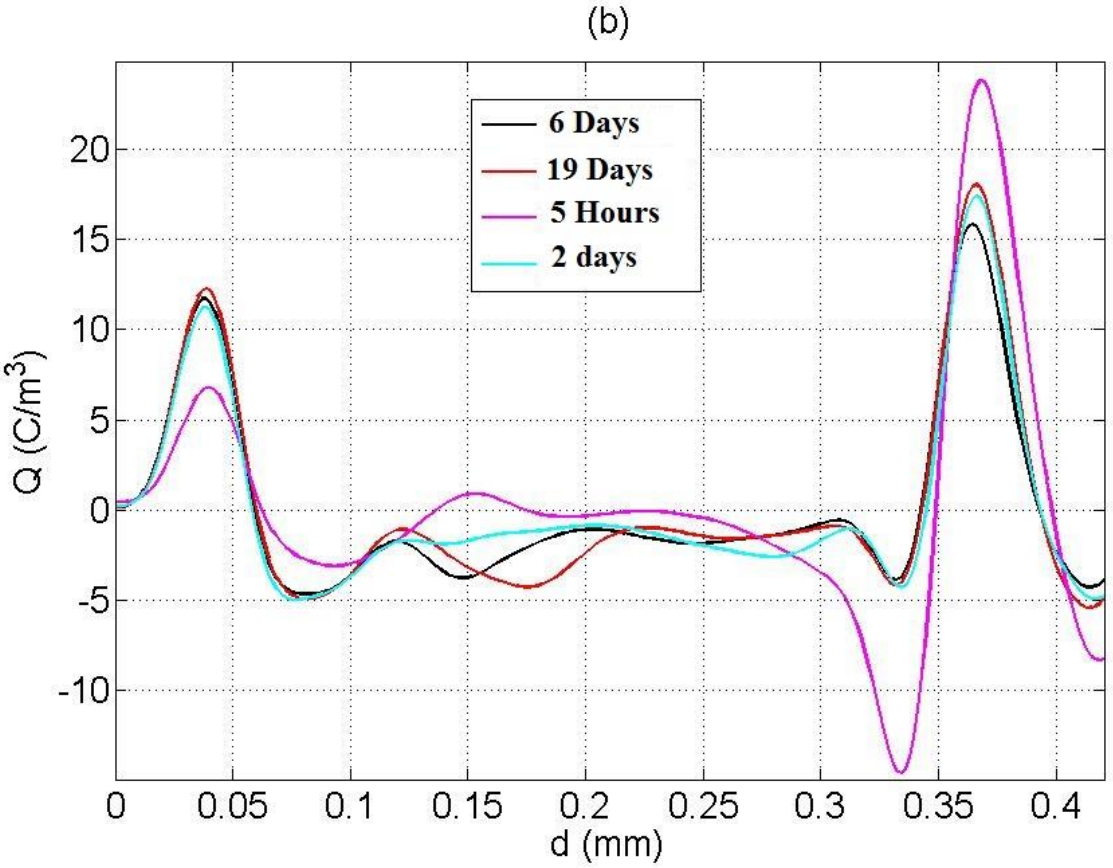

Figure 25: Space Charge Distribution Sample 3, Voff

4.3.2. Field Distribution

The field distribution shifts from having a stronger field on the cathode side to the field being stronger on the anode side.

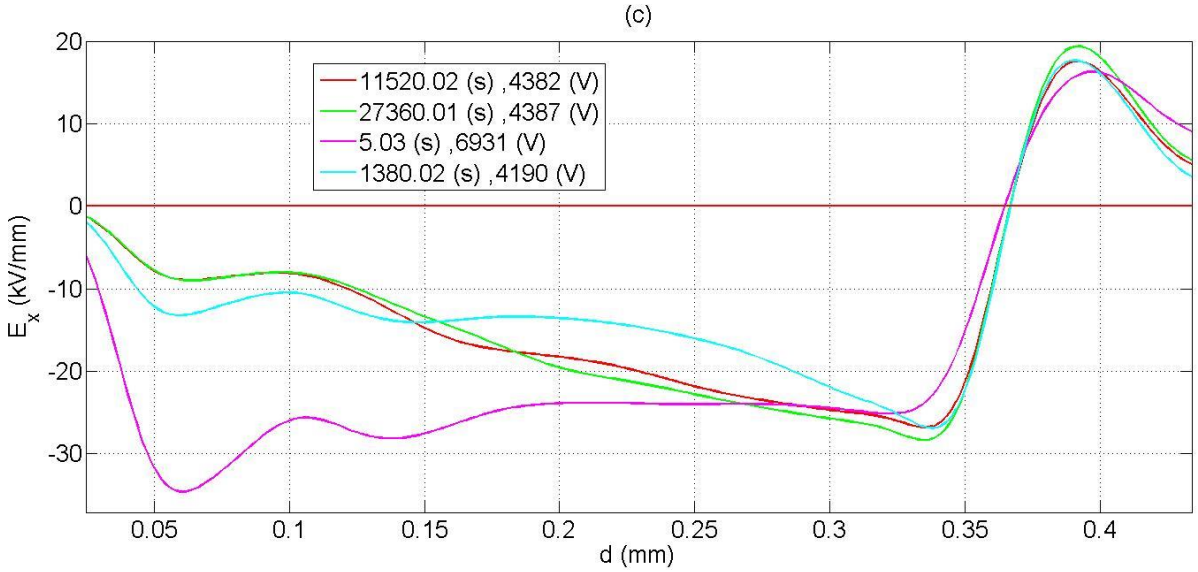

Figure 26: Field Distribution Sample 3, Von

The field also stabilises more or less in this distribution after 24 hours. There is, however, some difference between the distribution after 24 hours and the later measurements, with the field being slightly stronger on the cathode side, and slightly weaker in the rest of the bulk of the material. This reflects the difference seen in the space charge measurements as well.

When considering the field distribution with the voltage off, seen in *Figure 27*, the influence of the space charge on the field can be seen. The distribution of the field in the measurements after 24 hours and later mirrors the shift observed in *Figure 26*.

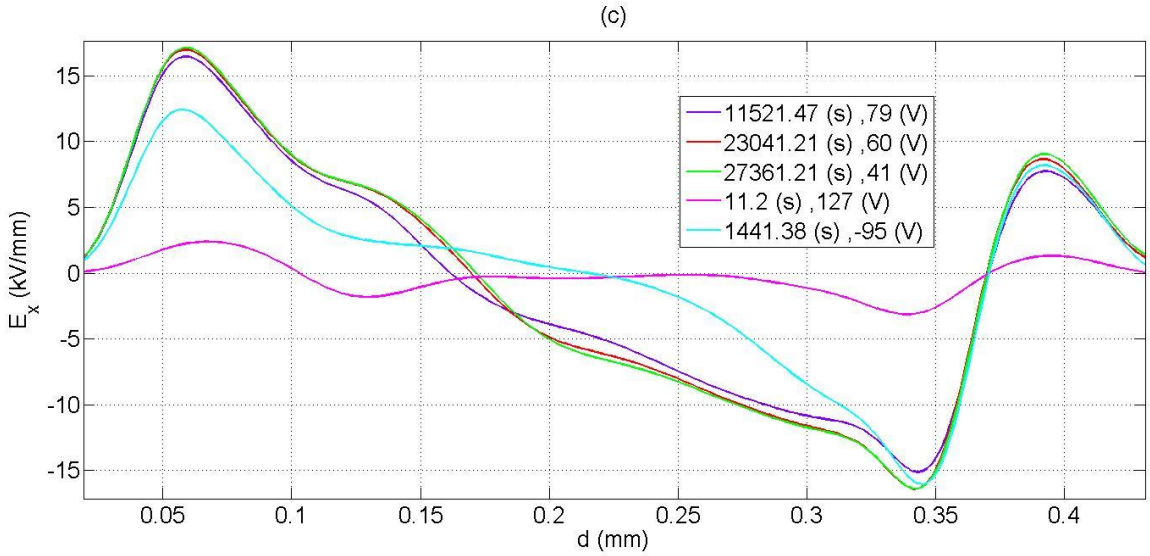

Figure 27: Field Distribution Sample 3, Voff

4.4. Sample 4

4.4.1. Space charge distribution

Sample 4 was produced as a single film of cross-linked polyethylene in order to examine whether the measurements would produce a significantly different result from the ones performed with layered samples. Since the results obtained with a voltage of 15kV were more significant than those obtained with a voltage of 10kV, while still having seemingly less noise than those obtained with 20kV, a voltage of 15kV was chosen for this sample as well. As can be seen in *Figure 28* and *29* the space charge distributions obtained were more erratic than those obtained from any of the other samples. Still, the accumulation of positive charge at the anode, and negative at the cathode are similar to what was seen in other samples.

Voltage on

The charge accumulation at the cathode peaks negatively at the first measurement, with -7.81C/m^3, sinks to -4.24C/m^3 after days, before increasing and ending at -4.87C/m^3 at the last measurement. The hetero charge present in the bulk by the cathode is at 4.63C/m^3 already by the first measurement, peaks at 5.24C/m^3 after 12 hours, and sinks down to 2.55C/m^3 by the last measurement.

The charge at the anode is stricktly increasing, starting at 4.42C/m^3, and ends at 20.77C/m^3 in the last measurement. The hetero charge close to the anode develops quickly during the first 2 days, up to -7.78C/m^3, and changing slowly during the rest of the period, with a measured charge of -7.26C/m^3 at the last measurement.

In these measurements as well, there are local peaks developing quickly in the bulk of the material, with little change happening after the first measurement. The negative charge around 0.28mm starts at -2.12C/m^3, and ends up at -2.55C/m^3. The positive charge around 0.365mm starts at 1.70C/m^3 and ends at approximately 0C/m^3.

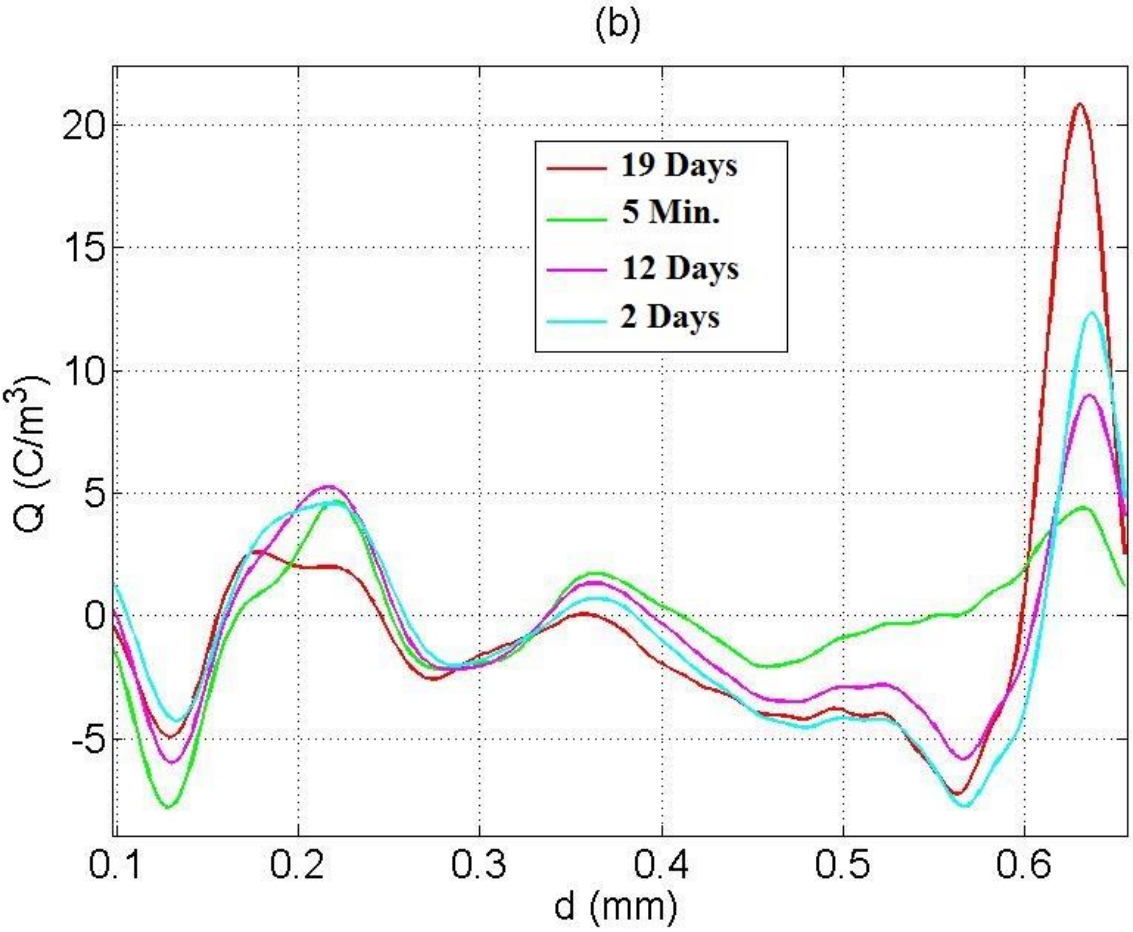

Figure 28: Space Charge Distribution Sample 4, Von

Voltage off

When considering the space charge distribution with the voltage off, there is a correllation with the voltage on measurements. The difference between the charge density in the first measurements and the later measurements is similar in *Figure 28* and *Figure 29.* Here as well, the development close to the electrodes is similar to that observed in sample 2, while the measurements in the mid-parts of the bulk appear to be noisy.

Both the hetero charge by the anode and the charge at the anode increase quickly during the first 2 days. The charge in the bulk by the anode reaches -5.44C/m by two days, and ends at -5.36C/m^3. At the electrode, the charge is up to 5.18C/m^3 after two days, and 8.67C/m^3 after 19 days.

The charge at the cathode starts out slightly negative, but is positive before 40 minutes have passed. The development here is positive during the whole period, with the rate of change consistently decreasing. The final and highest value for the charge at the cathode is 5.67C/m^3. There is homocharge present in the bulk close to the cathode after 2 days. This charge grows more negative as time passes, and ends up with a density of -2.60C/m^3.

In the central bulk, there is an accumulation of positive charge at the cathode side, and a negative accumulation at the anode side. Both of these are apparent after 2 days, and increasing in amplitude throughout the measurements. The positive accumulation ends up with a density of 1.28C/m^3, while the negative charge ends with -2.02C/m^3. Between the negative accumulation in the central bulk and the negative accumulation by the anode, the density shrinks to -0.72C/m^3 in the last measurement.

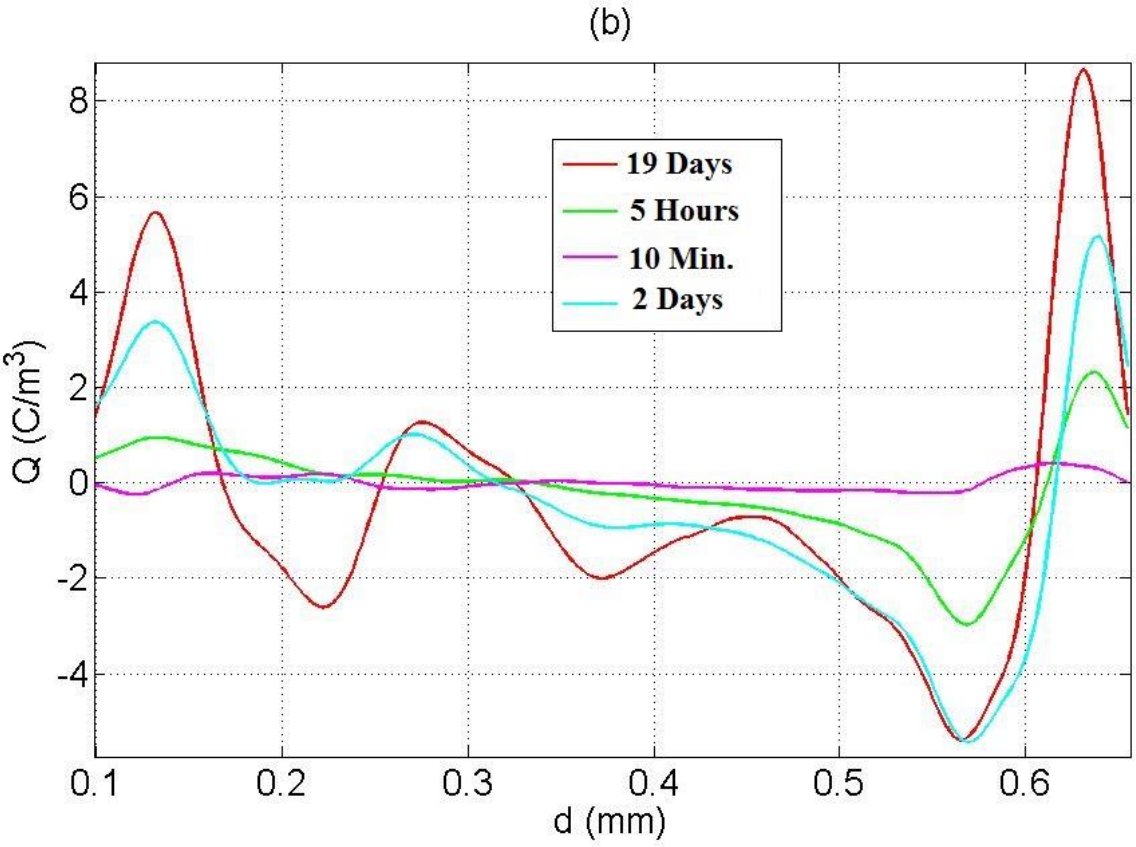

Figure 29: Space Charge Distribution Sample 4, Voff

4.4.2. Field Distribution

Voltage on

The measured field distributions with the voltage on has considerable amount of error which improves somewhat with time. When considering only the warping of the curve shape as charges accumulate, a similarity to what was observed in other samples can

be seen – as charges accumulate, the field on the cathode side shifts positively, while the field on the anode side shifts negatively.

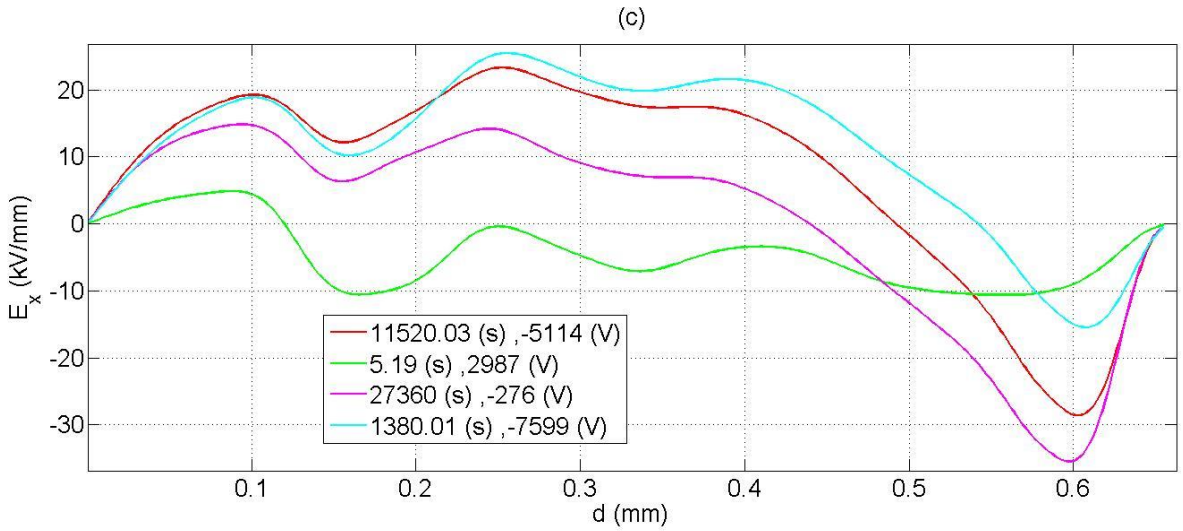

Figure 30: Field Distribution Sample 4, Von

Voltage off

The same can be observed in the voltage off measurements, with a considerable amount of error here, too. The error does diminish as time passes, but the positive component of the field distribution is consistently too large throughout the measurements, the first one notwithstanding.

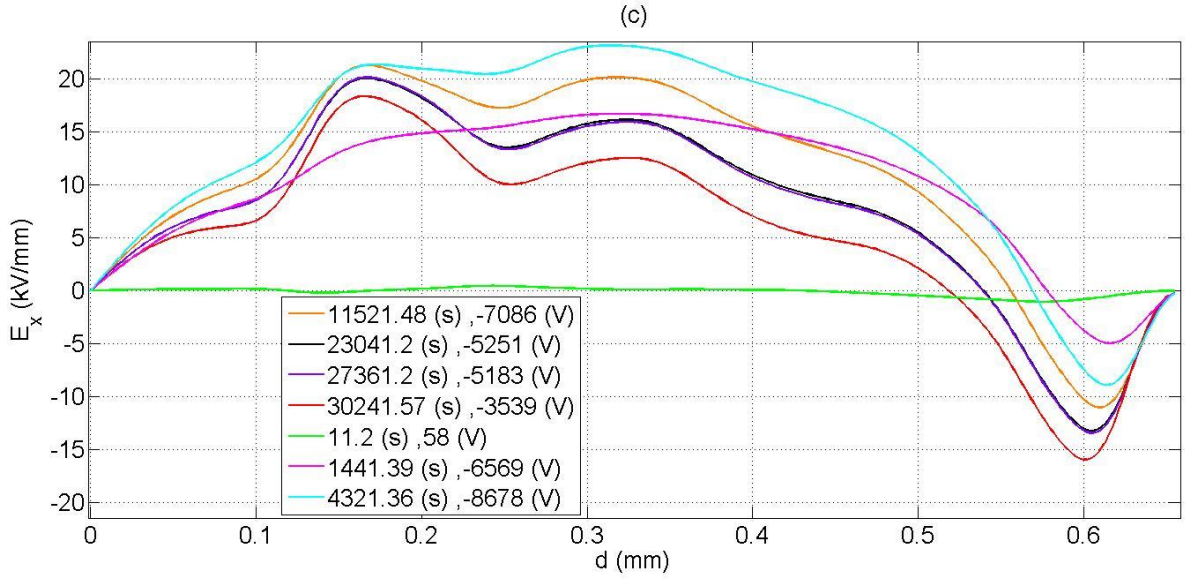

Figure 31: Field Distribution Sample 4, Voff

4.5. Sample 5

4.5.1. Space Charge Distribution

Voltage on

The charge at the cathode-polymer interface is at its maximum by the first measurement, reaching -13.83C/m^3. Its minimum of -5.95C/m^3 is reached by the last measurement. The accumulation is quite stable from the fifth day (-6.23C/m^3), with little change happening after this. The last measurements done on this sample were done after 8 days.

Hetero charge close to the anode quickly increases the first 16 hours up to a density of -8.40C/m^3, and reaches a maximum of -8.94C/m^3 after 2 days. The development is towards lesser density after this, and the measurements end at -7.01C/m^3. There is very little change after 6 days, though. Most of the increase in positive charge at the anode also takes place the first 16 hours, up to 16.68C/m^3. The maximum of 17.83C/m^3 is reached at the same time as the hetero charge, after 2 days. The last measurement shows a density of 16.96C/m^3, again with very little change the three preceding days.

The charge in the bulk is also in this case mostly negative, with a local minimum developing at 0.14mm, reaching a density of -2.34C/m^3, which is the same in both the last and second to last measurement.

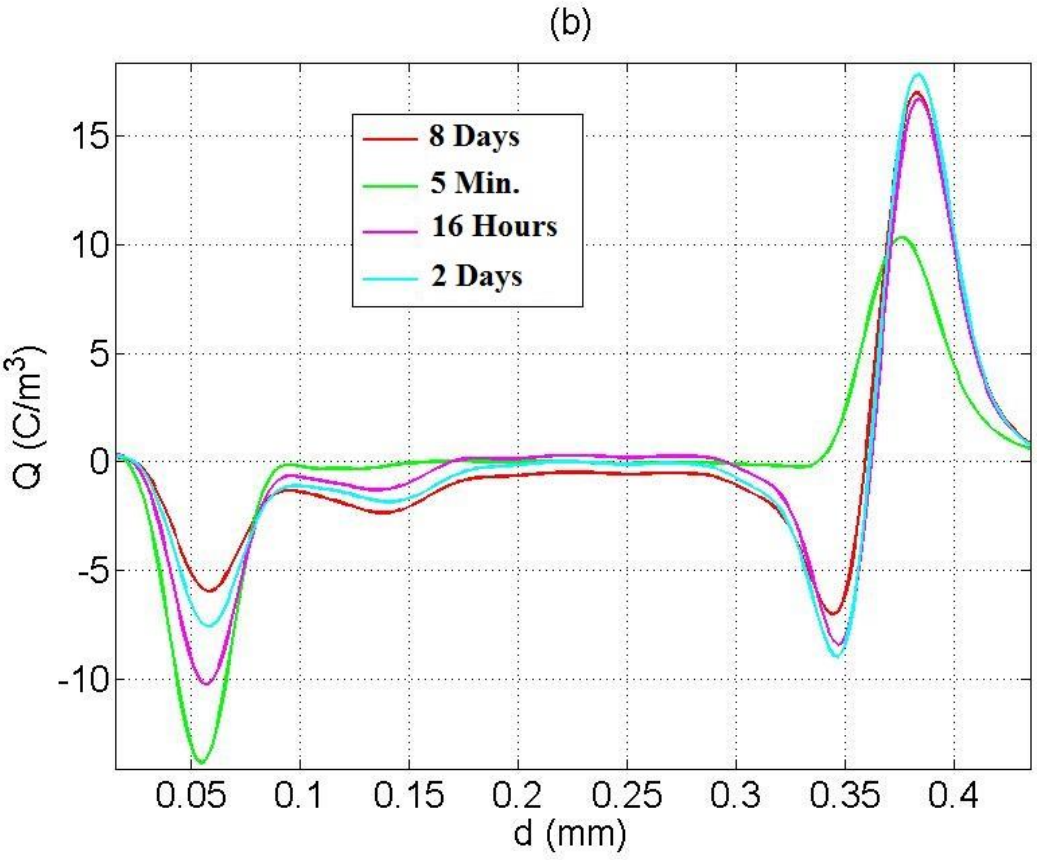

Figure 32: Space Charge Distribution Sample 5, Von

Voltage off

As would be expected from the voltage on measurements, the charge at the cathode-polymer interface is positive already by 5 minutes. The density increases quickly up to 7.21C/m^3 the first 2 days, and reaches 9.23C/m^3 by the 8th day. The development is very small from the 5th day, at 9.15C/m^3.

The hetero charge by anode the does most of its increase the first 16 hours, reaching a density of -10.92C/m^3. The maximum density of -12.56C/m^3 is reached after 2 days, and by the last measurement, the density is down to -10.93C/m^3. The positive charge at the anode follows close to the same pattern, reaching 8.77C/m^3 after 16 hours, then going up to 11.5C/m^3 after two days, and ending 11.92C/m^3. The maximum of 12.27C/m^3, however, is reached after 5 days.

The minimum in the bulk of the material close to the cathode reaches a maximum of -3.92C/m^3 by the last measurement, also here unchanged from the second to last measurement.

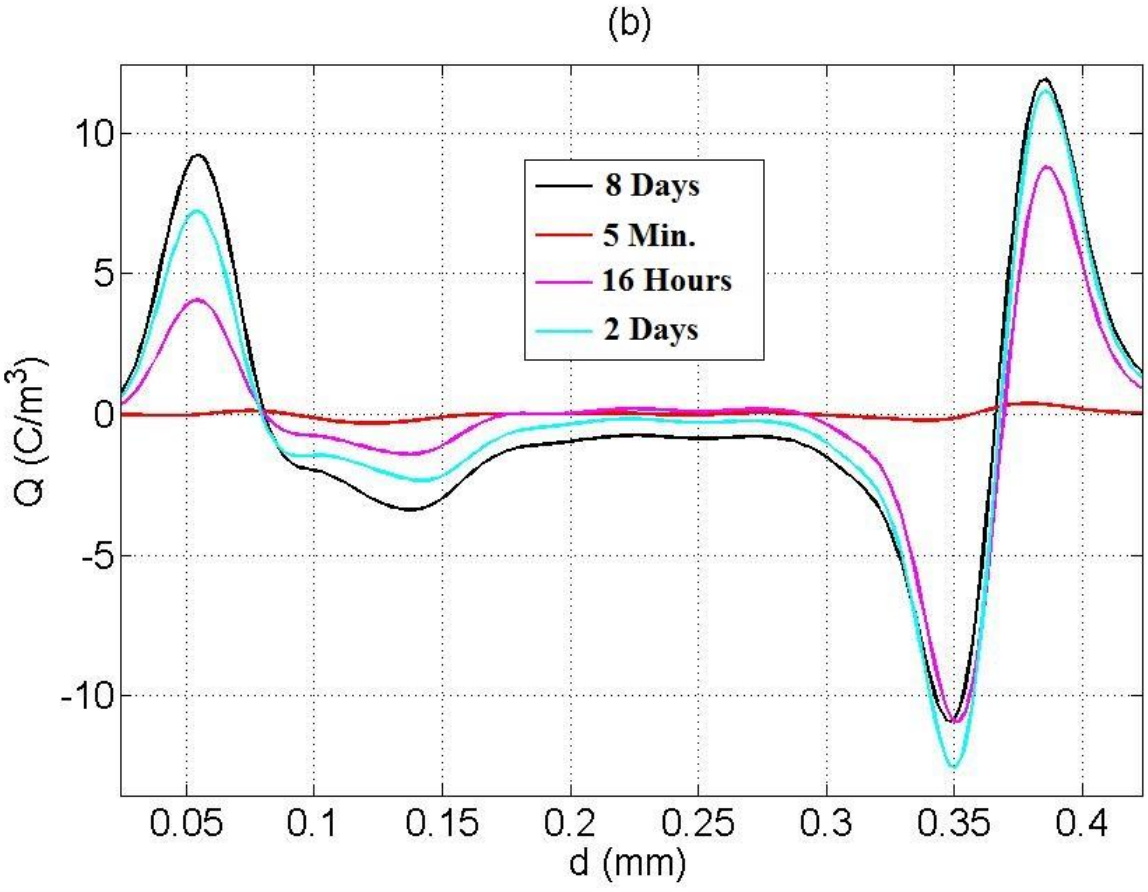

Figure 33: Space Charge Distribution Sample 5, Voff

4.5.2. Field Distribution

The same increase and decrease in field strength is seen here as in other samples, but with a more pronounced peak by the anode.

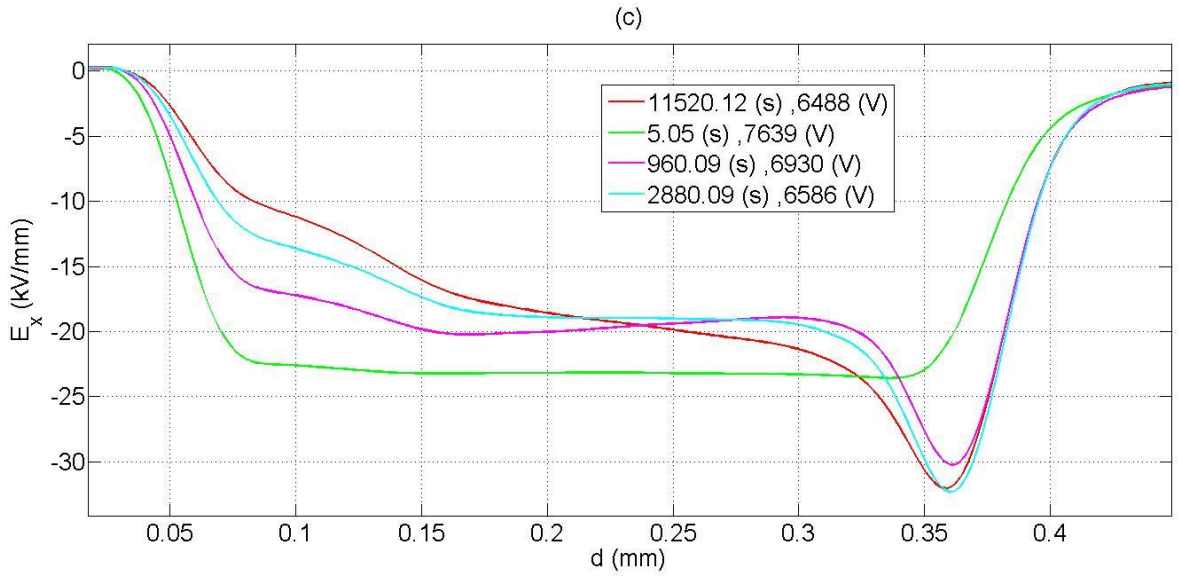

Figure 34: Field Distribution Sample 5, Von

The field with the voltage off also shows the characteristic positive field by the cathode and negative field by the anode. As in the voltage on field distribution, the peak by the anode is quite pronounced here.

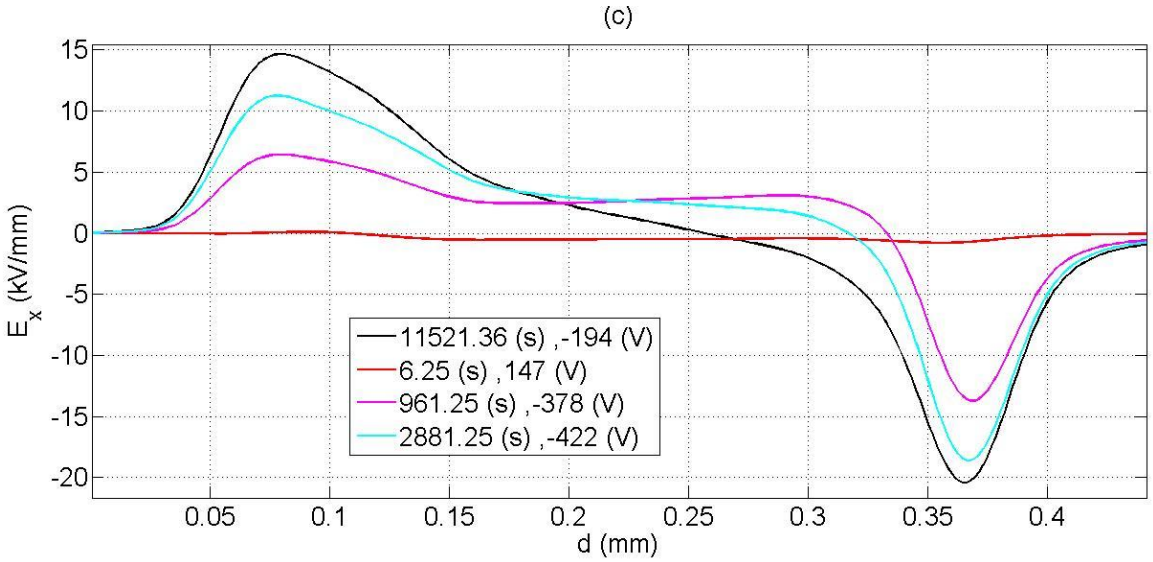

Figure 35: Field Distribution Sample 5, Voff

4.6. PEA Result Summary

In order to make the results more manageable, some key numbers are shown in *Table 4* and *5*, for the voltage on and voltage off measurements, respectively. It could have been sensible to add rows for time of stabilisation of the charge accumulations in the bulk close to the anode, and in the anode-polymer interface, but since there is no exact time of stabilisation, this was not done. The similar development of these two charge accumulations has already been mentioned where relevant. The measured field strengths are approximations from the initial graphed distributions, as are the field reduction and increase percentages.

Sample	S1	S2	S3	S4	S5
Voltage [kV]	10.00	15.00	20.00	15.00	15.00
Thickness [mm]	0.42	0.42	0.37	0.42	0.32
Q max Anode [C/m^3]	15.62	13.91	56.73	20.77	17.83
Q max Cathode [C/m^3]	-11.27	-14.64	-24.75	-7.81	-13.83
Q Cat, Last Measurement [C/m^3]	-5.79	-6.57	-6.20	-4.87	-
Q max Bulk Anode [C/m^3]	-3.00	-5.12	-13.90	-7.78	-8.94
Time Q max Anode	6 days	12 hours	12 hours	19 days	2 days
Time Q max Cathode	10 min.	80 min.	5 min.	5 min.	5 min.
Time Q max Bulk Anode	5 days	12 hours	6 hours	2 days	2 days
Avg. Field (calculated) [kV/mm]	24.02	35.71	54.57	35.71	46.63
Avg. Field (measured) [kV/mm]	13.50	17.00	18.07	24.50	23.30
Max Field Reduction [%]	40.74	41.18	56.12	40.82	57.08
Max Field Increase	61.70	37.71	56.23	44.69	39.48

Table 4: Numerical Summary of Results, Voltage On

Sample	S1	S2	S3	S4	S5
Voltage [kV]	10.00	15.00	20.00	15.00	15.00
Thickness [mm]	0.42	0.42	0.37	0.42	0.32
Q max Anode [C/m^3]	3.40	7.00	21.00	8.67	12.27
Q max Cathode [C/m^3]	9.89	3.73	11.09	5.67	9.23
Q Cat. Last Measurement [C/m^3]	9.16	3.73	11.09	5.67	-
Q max Bulk Anode [C/m^3]	-3.57	-6.57	-12.17	-5.44	-12.56
Time Q max Anode	8 days	3 days	7 hours	19 days	5 days
Time Q max Cathode	15 days	19 days	19 days	19 days	8 days
Time Q max Bulk Anode	5 days	24 hours	6 hours	2 days	2 days

Table 5: Numerical Summary of Results, Voltage Off

4.7. Crystallinity of the Samples

The crystallinity of layered samples and homogeneous samples was measured using DSC in order to examine whether or not the layers of the layered samples have different conductivity. Two different time and temperature settings were used in order to measure the crystallinity. The melting curve of the samples when a longer timespan was used to heat the samples can be seen in [A.IV.a], while the melting curves obtained with a quicker heating can be seen in [A.IV.b]. The degree of crystallinity of single-layered samples is measured as higher in both, but only 0.33% and 1.36%, respectively. This indicates that there is little difference in conductivity between the layers.

Chapter 5

Discussion

The measurements performed on layered samples of cross-linked polyethylene were intended to examine whether cable joints present a potential risk for accumulation of space charge. The conditions in cable joints were recreated as accurately as possible with the chosen method of investigation – samples of double cross-linked material linked with cross-linked material were produced, and examined through the PEA measuring method.

Three different voltage levels were chosen: 10kV, 15kV and 20kV. With the samples having an estimated thickness of approximately 0.5mm, these levels would amount to fields of 20kV/mm, 30kV/mm and 40kV/mm. In reality, the thickness of the samples varied greatly, leading to fields of 24kV/mm, 35kV/mm, 54kV/mm, 35kV/mm and 47kV/mm for sample 1, 2, 3, 4 and 5, respectively. One series of measurements was performed at each of the voltage levels, except for at 15kV, where measurements were performed on two samples. Each of the samples, except for sample 5, was placed under stress for time periods of 19 days, and the measurements were performed in time intervals as shown in [A.II]. Voltage was applied to sample 5 for no more than 8 days, due to a lack of more time. In addition to the measurements performed on the layered samples, a voltage of 15kV was applied to sample 4, which consisted of only one layer of cross-linked material. This was done in order to examine whether or not there would be any significant difference between the accumulation of space charge in such a sample and the layered samples.

As a final measure aimed to aid in the explanation of the observed results, the crystallinity of the samples was measured using DSC. Though not the most accurate method of investigating the conductivity of the layers, these measurements could possibly give an indication as to whether the difference of conductivity was large enough to influence the accumulation of charge in the samples.

5.1. Space Charge Distribution and Development

For all of the samples examined, the shape of the charge distribution, as well as its development remained similar in the areas close to the electrodes, indicating a specific behaviour of LE4253DC in combination with AU electrodes under the stress conditions examined.

The recurring shape of the charge distribution for voltage on and off conditions by the final measurement is illustrated in figure 36:

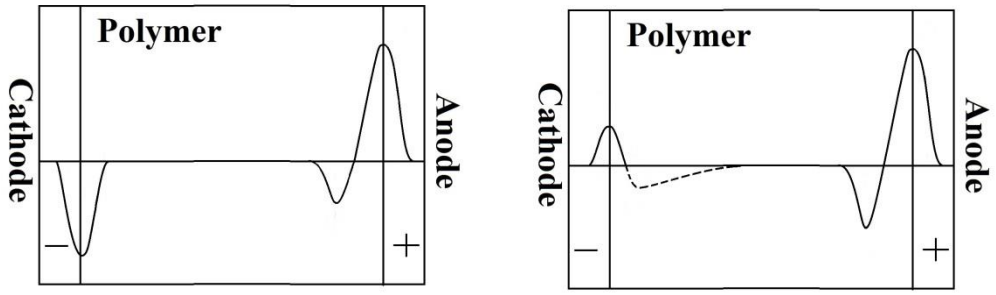

Figure 36: Characteristic Final Charge Distribution Von and Voff

5.1.1. Charge development in the Vicinity of the Electrodes

In the first voltage off measurements on sample 1 and 2, homo charge is present in the electrode-polymer interfaces. The homo charges at the cathode quickly develop into hetero charges. A stronger field leads to a faster transition, and in sample 3, 4 and 5, the charge is positive already by the first measurement.

Parallel with the homo charge developing at the anode-polymer interface, hetero charge accumulates in the polymer bulk close to the electrode.

It appears that the rate of transport exceeds the rate of injection at the cathode, when considering the accumulation of hetero charge the anode and the accumulation of positive charge at the cathode interface. If positive charge has a low rate of extraction and recombination at the cathode, at the same time as electrons are quickly transported away, the results would be accumulation of positive charge at the cathode.

The hetero charge accumulation in the bulk close to the anode indicates that the rate of extraction at the anode is lower than the rate of injection from the cathode. In the voltage off measurements of sample 1, 2, 3 and 5, the positive anode charge and the anode bulk hetero-charge reach their maximum values and stability at approximately the same time, indicating saturation of charge, and possible recombination and extraction. A probable explanation is that as the field is strengthened due to the hetero-charges, it becomes easier for electrons to be extracted, and as the rate of extraction and injection coincide, equilibrium is reached. Though the field distributions obtained from the measurements are not correct in magnitude, the strengthening of the field by the anode is clearly visible. It can also be seen that the shape of the field distribution changes little after the charge accumulation has stabilised by the anode.

The development of the charge accumulations, as mentioned, is sped up as the field is increased, both by the cathode and the anode. This is in correlation with *Schottky*

charge injection, where the energy barrier for injection and extraction in reduced as the field increases. The conductivity of the material also increases with the field, allowing the charges to travel from one electrode to the other faster. Similarly to the *Schottky* effect, according to the *Poole-Frenkel mechanism,* a higher field lowers the potential barriers between traps in the dielectric bulk, assisting electrons in their travel from the cathode to the anode via thermally-activated hopping [1].

According to [1], the threshold for *Schottky injection* is 10kV/mm, which is well below the fields applied in this work. The other mode of injection discussed in Section 2.6.4, *Fowler-Nordheim injection*, is only dominant with an applied field upward of 100kV/mm. As the maximum field applied to a sample in this work is approximately 40kV/mm, *Fowler-Nordheim injection* is thus an unlikely candidate for the explanation of the results obtained here.

In [1] it is suggested that peaks of hetero charge close to electrodes may be caused by partial alignment of permanent dipole molecules from impurities and additives. The samples used in these experiments have been thermally pre-treated for three days in order to reduce the amount of residuals. It does not seem like there are enough dipoles to have a significant impact, given that there is no sign of permanent dipoles in the bulk close to the cathode.

Impurities may however contribute in the form of field assisted ionisation of chemicals. These ions migrate towards the electrode of opposite polarity, but cannot be extracted once they reach the electrode-polymer interface, since the charge migration is a form of mass transport. Ions therefore contribute with hetero charge at the electrodes. The contribution of ions is difficult to estimate precisely, since they can be present in the midst of charge of the opposite polarity. The PEA measurements only indicate the sum of charge in an area, leaving no definite information about the constituent parts of a charge accumulation.

5.1.2. Space Charge Accumulation in the Central Bulk

In the middle part of the bulk of the material, the general trend of the measurements is an accumulation of negative charge. However, differences in the shape of the curves in this area make it difficult to say anything more conclusive about the general behaviour of charge in the central parts of the bulk. The general trend towards negative charge in the bulk may indicate that there are more traps for electrons in the polymer, though. With regards to the question these experiments aimed to answer, there is no obvious evidence of influence from the interface between the two layers of polyethylene on the accumulation of charge.

Moreover, the differences observed in the charge accumulation in the central bulk area, indicate that individual differences in the morphology of the samples may be

quite influential in the accumulation of space charge. This conclusion was also reached in [2].

The measurement of the crystallinity of the samples indicated little to no difference in the crystallinity of the double cross-linked layer compared to the cross-linked layer, thus also indicating little difference in conductivity. With no real difference in the conductivity of the layers, a possible cause for space charge accumulation could have been an increased number of traps in the interface. There could have been more regions of amorphous material and crystal defects in the interface area due to incomplete crosslinking. Since traps are related to the concentration of residuals from additives, and residuals tend to be more common in amorphous regions [3], this could lead to charge accumulation. As mentioned, the crystallinity of the samples was close to identical, and there was no evidence of charge accumulation in the interface, thus indicating that incomplete crosslinking is not a worry in this regard.

5.2. Field Distribution

In all of the samples, the charge distribution contributes to a weaker field on the cathode side, and a stronger field on the anode side. The field distortion is present after not much time, and is as expected from the observed accumulation of hetero charge by the anode. Though the absolute values of the field measurements are not trustworthy, the shape also gives an indication of percentagewise increase in field intensity. The greatest distortion of the field was observed in sample 1, where an approximate calculation indicated a field increase of 62%, a value which is probably too large, judging from the field distribution with the voltage off. The distribution with the voltage off is heavily biased negatively on the anode side, with an obviously negative total field across the sample instead of a neutral total field as would be correct. Nevertheless, even if exaggerated, the increase in field strength could heavily influence the lifespan of the insulation negatively. With regards to the variation in space charge in the bulk of the material (apart from the hetero charge by the anode), no significant influence on the field could be seen.

5.3. Variations between Measurements of Samples with an Applied Voltage of 15kV

As mentioned, there appears to be large individual differences between the samples, evidenced by the different charge distributions in the central bulk of the samples. Other differences are accentuated when considering the space charge accumulations of sample 2 and 5, which had the same voltage applied. Sample 2 is thicker than sample 3, and accordingly has a weaker field. It therefore makes sense that with the voltage on, the maximum charge density at the cathode of sample 5 is reached faster than in sample 2. The development of charge at the anode is slower in sample 3, but this may

be because the charge reaches a higher density. With the voltage off, the faster development of sample 5 is more evident, and the density of charge is higher in all areas. With a difference in field strength of 10kV/mm, it is difficult to make more valuable observations, and a comparison between sample 2 and 4, which had almost identical field strength, could be more valuable. The problem with this is the fact that the measurements for sample 3 were very erratic, in all probability due to weak contact between the electrodes of the PEA system and the sample (see section 5.4). Still, the magnitudes of the accumulations at the electrode interfaces and the hetero charge by the anode are not too different. This indicates that though the distribution of charge in the bulk is very dependent on the morphology of the individual samples, the accumulation by the electrodes may vary to a lesser degree.

5.4. Sources for Error

Vibrations, temperature variations and influence from other equipment in the lab, are all possible sources for disturbance of the PEA measurement system. Noise was particularly prominent in sample 3 and 4, something which can probably be attributed to weak acoustic contact to between the electrodes and the sample. The brass electrode has to be manually adjusted, and after sample 4 was removed, the brass electrode seemed less protruding than it should be. The electrode was adjusted before sample 5 was inserted, and none of the problems associated with sample 3 and 4 were present in the measurements of sample 5.

Chapter 6

Conclusion

Based on the results obtained in this work, there is no increased risk of space charge accumulation in the interface between cross-linked and double cross-linked polyethylene of the same material. Measurements of the degree of crystallinity indicated little difference in the conductivity of the layers, explaining in part why there was no accumulation of charge in the interface. Charge could have accumulated due to of incomplete crosslinking and defects in the interface, but the lack of charge indicates that this should not be a worry.

Hetero charge accumulates rapidly in the polymer by the anode, and leads to a significantly increased field strength in the vicinity of the anode. As the field is increased, the rate of extraction is increased, due to a lowering of the potential barrier. The accumulation and extraction thus reach a state of equilibrium, stabilising the charge accumulation. Still, the field increase could lead to accelerated ageing of the polymer, and, in the worst case scenario, breakdown of the material.

The accumulation of charge in the rest of the bulk of the material varies greatly from sample to sample, in all probability due to individual differences in morphology. The general trend is towards negative charge in the material bulk, indicating more traps for electrons.

Ions in the material could also represent part of the accumulation of charge observed, but since the measurements only show the sum of charge present in an area, it is difficult to judge the degree to which this could be the case.

Chapter 7

Further Work

If further measurements of the same character as the ones in this work were to be done, it would be recommended to run the measurements for a shorter amount of time, so that more measurements could be done at each voltage level. Though the whole course of the charge development takes more time, if the measurements are run just past the maximum

Further measurements on layered samples identical to the ones produced in this work do not seem to be of the greatest interest, but a larger selection of measurements would reduce the amount of doubt associated with the PEA system. A larger selection of measurements on samples consisting purely of cross-linked LE4253DC, could also give statistically more significant information on the general development of charge at the electrodes, and the variation from sample to sample.

Performing measurements with electrodes of a different material could also yield interesting results, as the rate of injection and extraction varies a lot depending on the combination of electrode and polymer material.

Changing the polarity of the voltage applied to a sample could give information about the transport of charge in the material, and whether there is any cause for worry in relation to this.

It would be recommended that extra care is taken that proper acoustic contact is established between the electrodes and the sample when performing further measurements with the PEA system. The shims used should also be measured carefully when producing samples in order to avoid variations in sample thickness.

References

[1] Giovanni Mazzanti & Massimo Marzinotto, “Extruded Cables for High Voltage Direct-Current Transmission”, Advances in research and Development, IEEE Press, Wiley, 2013

[2] Jens Eirik Hagen, “Romladningsdistribusjon i Lagdelt XLPE HVDC Kabelisolasjon”, Master’s Thesis, NTNU, June 2014

[3] L.A. Dissado, J.C. Fothergill, “Electrical Degradation and Breakdown in Polymers”, The Institution of Engineering and Technology, London, UK, 1992

[4] E. Ildstad, “High Voltage Insulation Materials", Dept. Elect. Eng., NTNU, Trondheim, Norway, Aug. 2012

[5] T. Kanno, T. Uozumi, and Y. Inoue, “Measurement of Space Charge Distribution in XLPE at High Temperature”, IEEE Int’l. Sympos. Electr. Insul., pp. 85-88, 1998

[6] F.H. Kreuger, “Industrial High DC voltage”, Delft University, Delft, Netherlands, 1995

[7] Kwan Chi Kao, “Dielectric Phenomena in Solids: with emphasis on physical concepts of electronic processes", Computer Engineering University of Manitoba, London, UK, 2004.

[8] B. Sanden,”XLPE cable insulation subjected to HVDC stress”, Ph.D. dissertation, Dept. Elect. Eng., NTNU, Trondheim, Norway, Nov. 1996

[9] H. ZHENG et al., “Inuence of cable clamping force on PEA measurements on HVDC mini-cables” in 2013 IEEE International Conference Solid Dielectrics, Bologna, Italy, June 30 - July 4, 2013

[10] F. Rogti, M. Ferhat, “Maxwell-Wagner polarization and interfacial charge at the multilayers of thermoplastic polymers”, in Journal of Electrostatics, 72, 2013 - 91 - 97

[11] Chen, G, Chong, Y L and Fu, M(2006) “Calibration of the Pulsed Electroacoustic Technique in the Presence of Trapped Charge”, Measurement Science and Technology, 17(7), 1974-1980

[12] G. Chen, Y. Tanaka, T. Takada, L. Zhong “Effect of Polyethylene Interface on Space Charge Formation", IEEE Transactions on Dielectrics and Electrical Insulation, Vol. 11, No. 1; February 2004, School of Electronics and Computer Science, University of Southhampton, UK.

[13] R. Bodega, “Space Charge Accumulation in Polymeric High Voltage DC Cable

Systems," Ph.D. dissertation, Delft University, Delft, Netherlands, 2006.

[14] G. C. Montanari and L. Simoni, "Aging phenomenology and modelling," IEEE Trans. Elect. Insul., vol. 28, pp. 755–776, Oct. 1993.

[15] Fabiani, D. ; Montanari, G.C. ; Laurent, C. ; Teyssedre, G. ; Morshuis, P.H.F. ; Bodega, R. ; Dissado, L.A. ; Campus, A. ; Nilsson, U.H. "Polymeric HVDC Cable Design and Space Charge Accumulation. Part 1: Insulation/Semicon Interface", Electrical Insulation Magazine , IEEE Volume: 23 , Issue: 6

[16] GSM industries 2009. Plastic Extruder Machinery, *http://www.gsmindustries.co.in/pages/products/plastic-extruder- machinery.html*

[17] TechImp Systems, "PEA FLAT SYSTEM", Operator's Manual, TechImp

[18] B. Wunderlich, M. Dole; "Specific Heat of Synthetic High Polymers. VII: High Pressure Polyethylene", J. Polym. Sci., Vol. 24, pp. 201-213, 1957

[19] Jens Eirik Hagen, "Romladningsdistribusjon i XLPE HVDC kabelisolasjon", Prosjektoppgave, NTNU, December 2013.

Appendices

I. Examples of Measurement of Sample Width

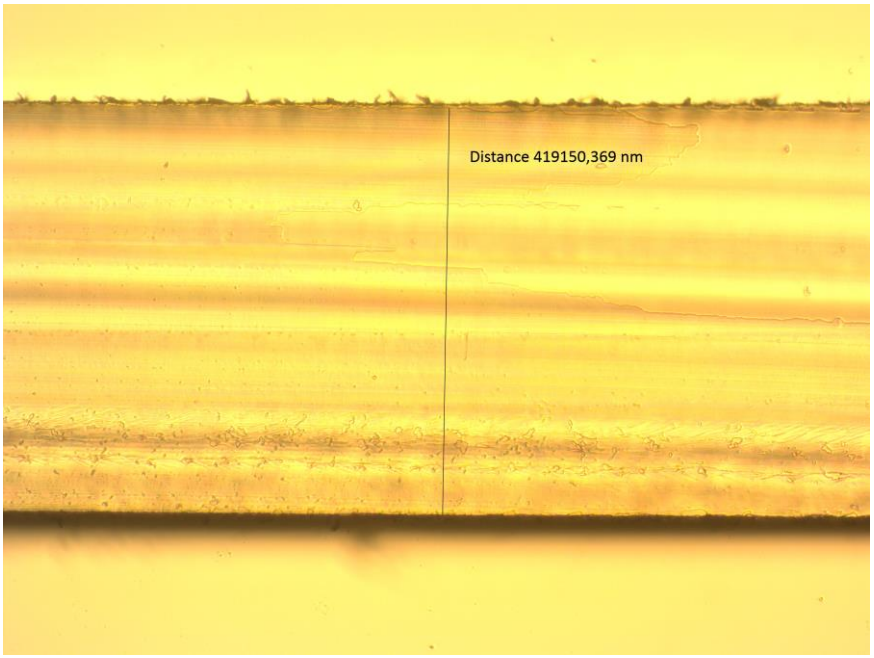

Sample 1, Measurement a

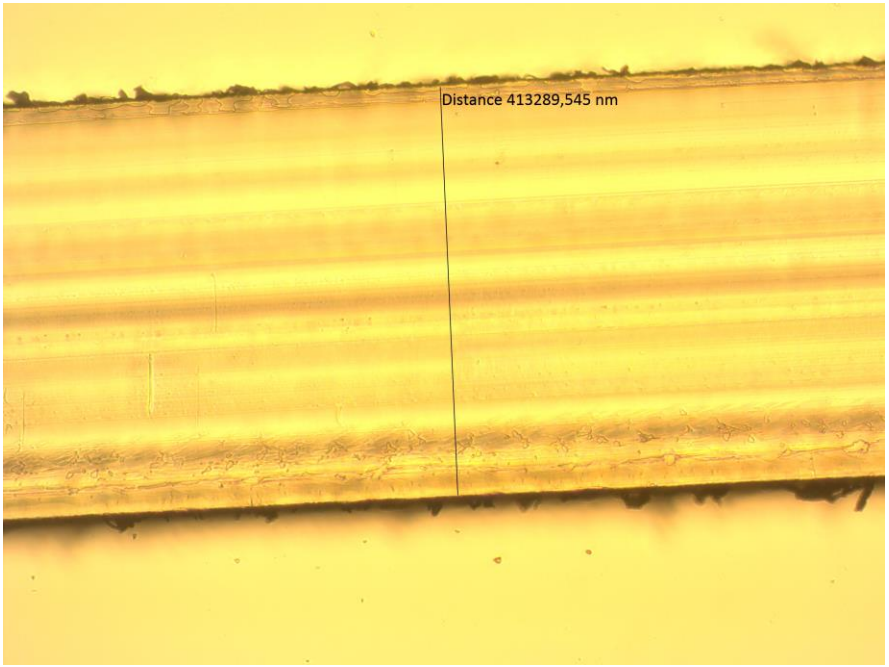

Sample 1, Measurement b

II. PEA Measurement Intervals

Time of Measurements [minutes]
5
10
15
40
80
100
120
150
180
240
300
360
420
480
540
600
660
720
780
840
960
1020
1080
1140
1200
1260
1320
1380
1440
2880
Further measurements were made once every 24 hours

III.Calibration Signals

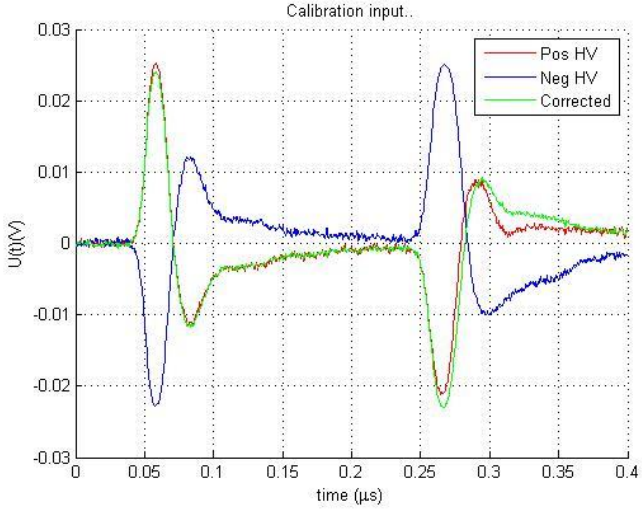

Calibration Signal, sample 1

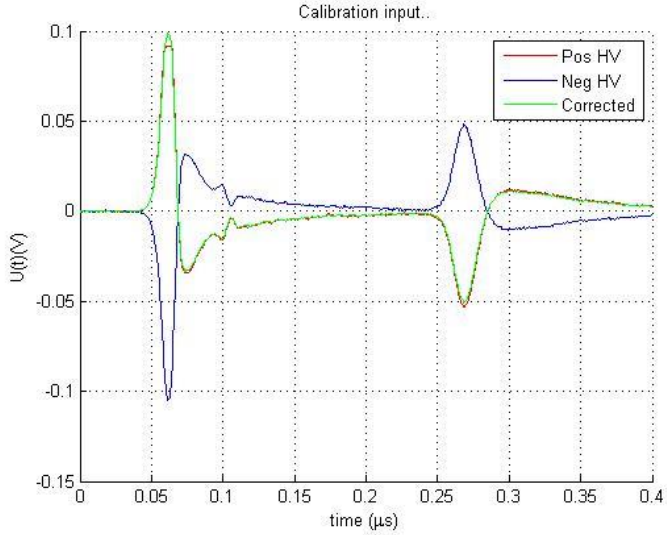

Calibration Signal, sample 2

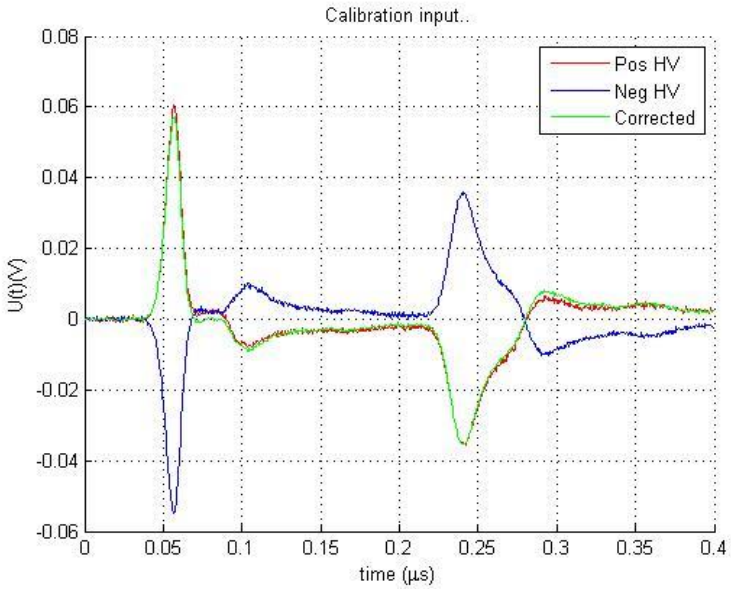

Calibration Signal, sample 3

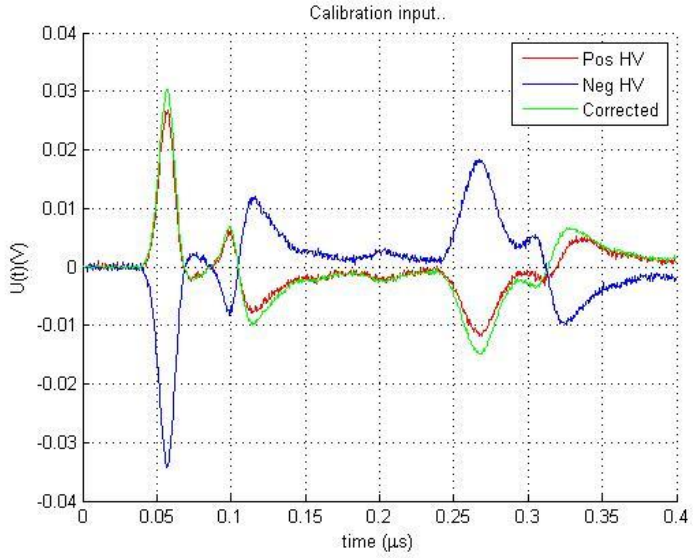

Calibration Signal, sample 4

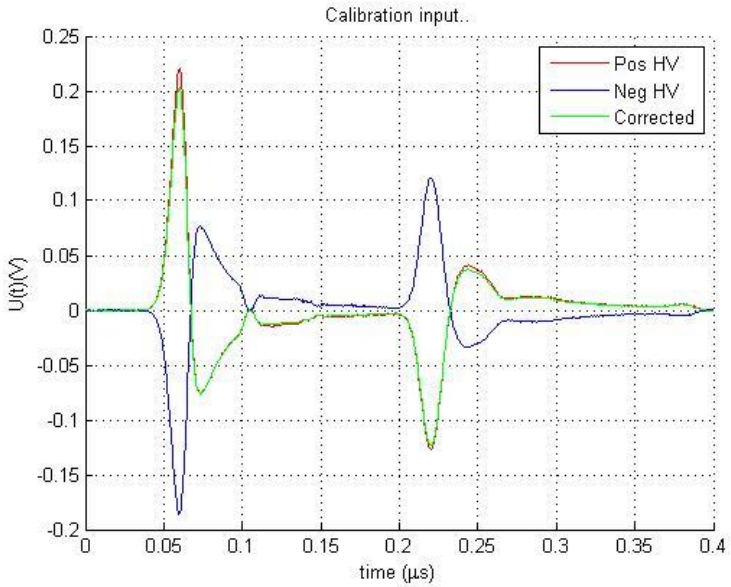

Calibration Signal, sample 5

IV. Illustrative Photographs

IV. a. Extrusion

Extruder

Water cooled drums

Polyethylene film on drum

IV. b. Moulding and Sample

Moulds and shim

Moulding Press

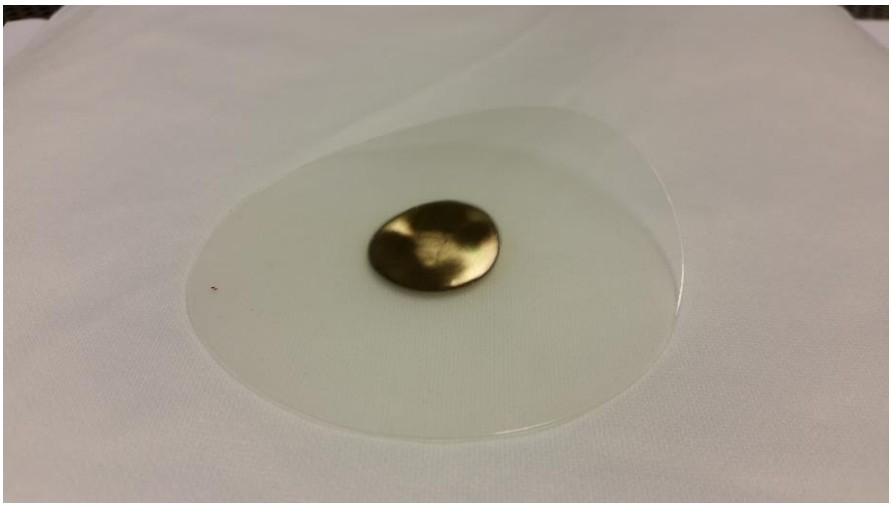

Finished Sample with Electrodes

IV. c. PEA Measurement System

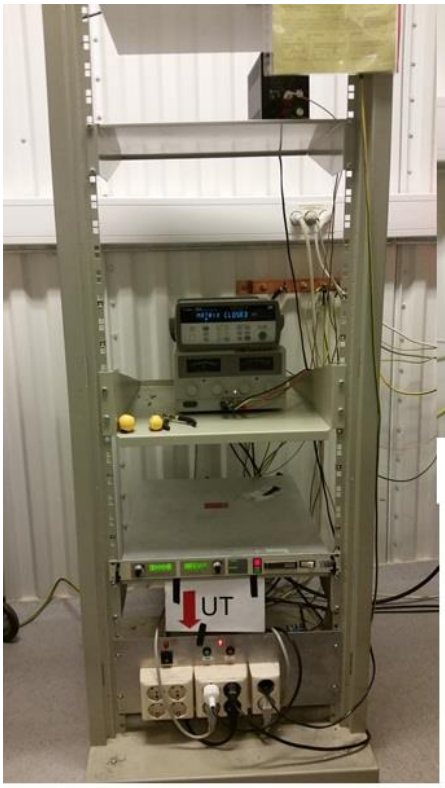

Source and signal generator

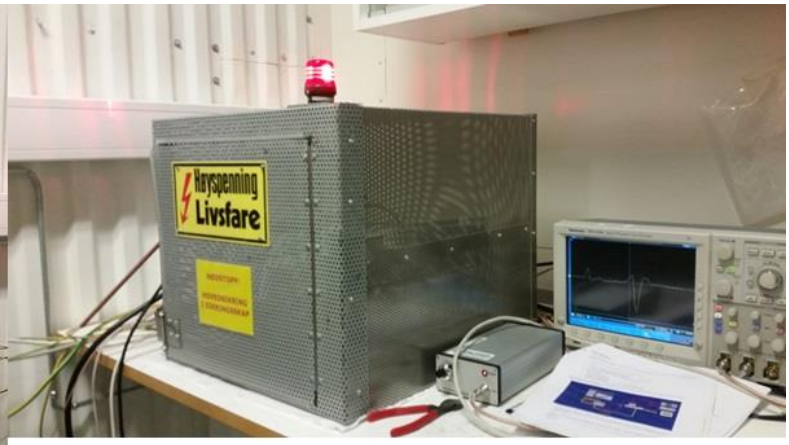

Faraday cage for measurement cell & oscilloscope

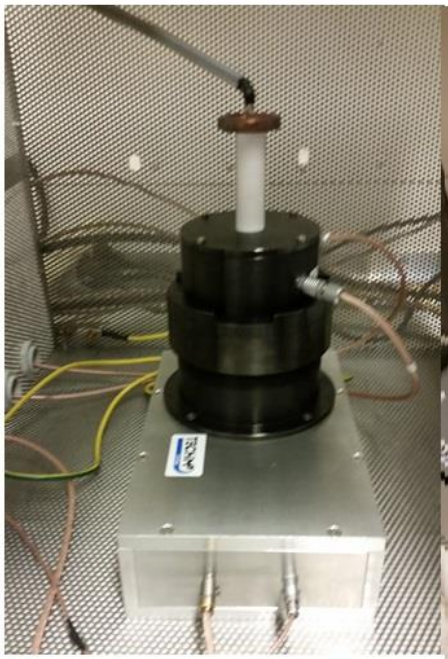

Measurement cell in cage

Measurement cell with sample inside

V. Melting Curves

V.a. Slow Program

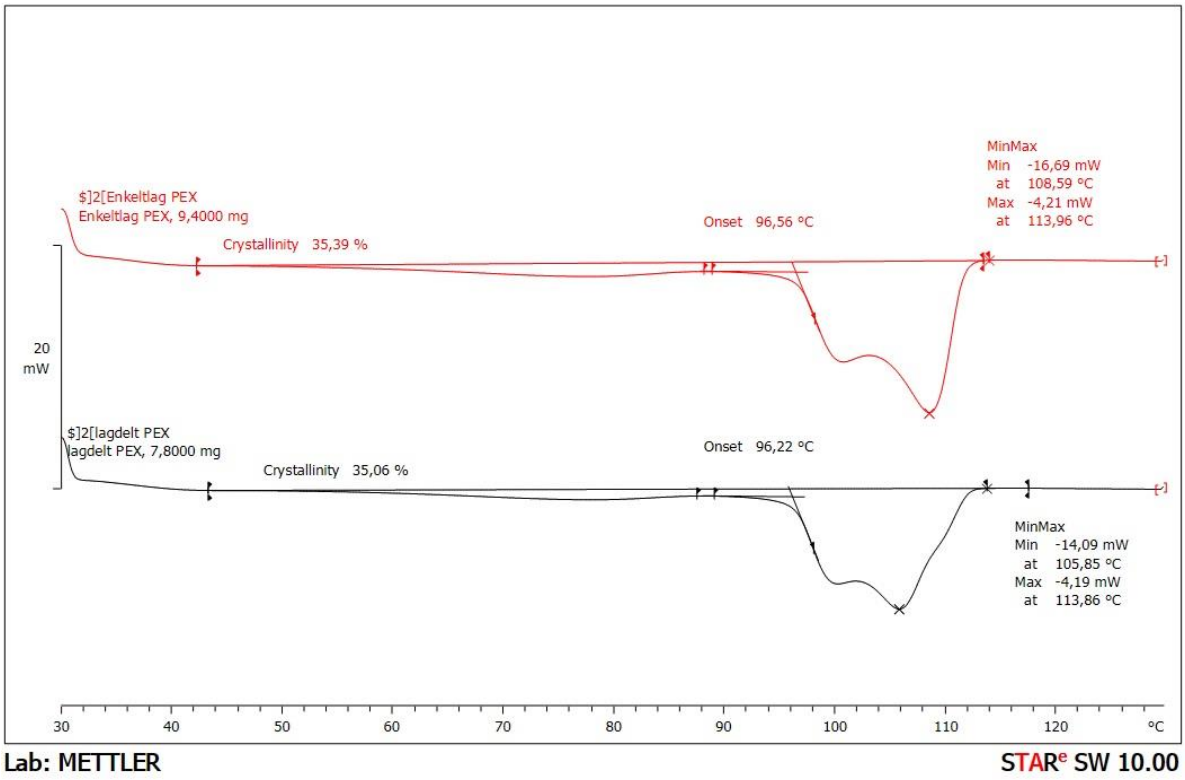

Melting curves of single layered (red) and double layered XLPE samples, slow program

V.b. Fast Program

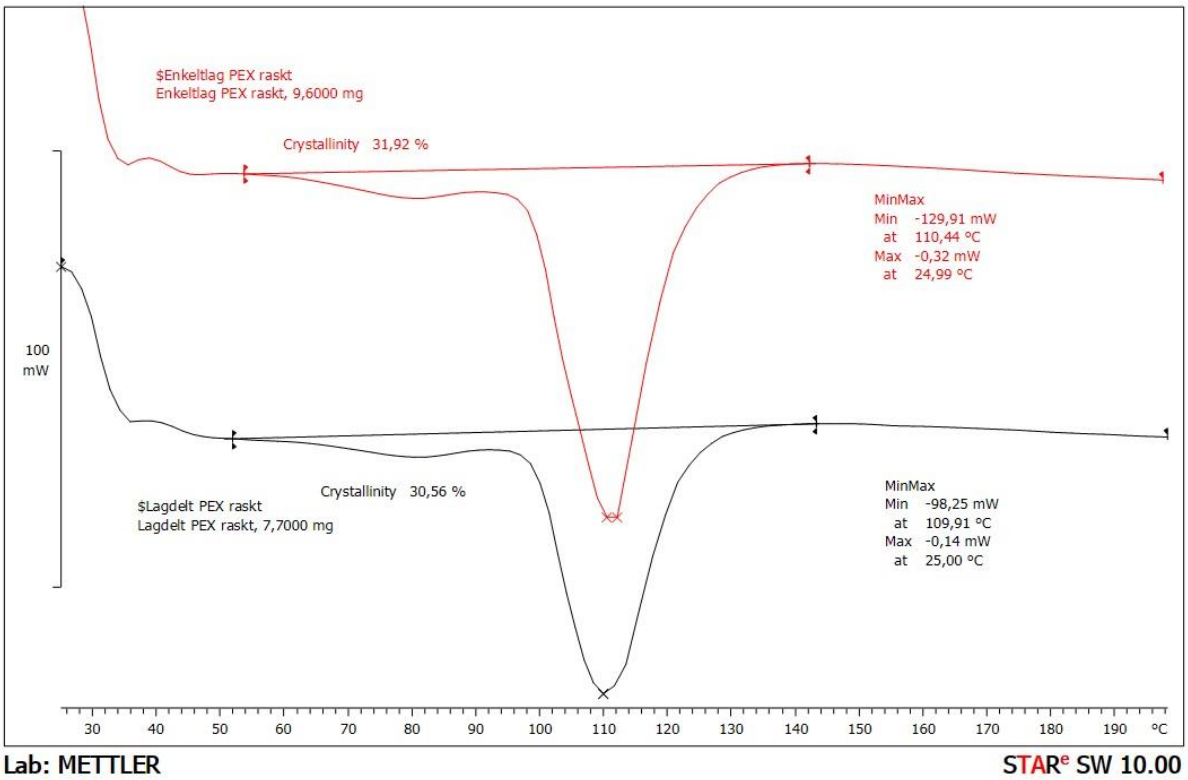

Melting curves of single layered (red) and double layered XLPE samples, fast program